# Beyond *cyp51*: A novel reduced spore dormancy pathway confers azole resistance in *Fusarium graminearum*

By
Kelsey Wog

A thesis submitted to the Faculty of Graduate and Postdoctoral Studies of The University of Manitoba in partial fulfillment of the requirements of the degree of

MASTER OF SCIENCE

Department of Microbiology

University of Manitoba

Winnipeg

# Acknowledgements

I would like to thank Dr. Matthew Bakker for your guidance, expertise, endless patience and kindness throughout this project. I would also like to thank Dr. Aleeza Gerstein for all your help with introducing me into the coding and stats world, your guidance in my project, and for our chats about life, reassuring me that I will be able to find my way in the unknown that the future holds. Thanks to you both for supporting and being patient with me while working on my project and taking my career in sport to the Olympic Games for the second time. Thanks to my committee members Dr. Sean Walkowiak and Dr. Ivan Oresnik for providing feedback on my project.

Thank you to my family, friends, and boyfriend for always entertaining my conversations about *Fusarium*, and to my social media following for playing along with my weekly Fungi Friday posts. Thanks to my fellow lab mates for being amazing humans to work with; you all are fantastic.

# Contribution of authors:

Wog, Kelsey: Conducted the experiments, collected data, analyzed the results and organized the manuscripts findings.

Bakker, Matthew G: Main supervisor. Provided guidance through the project including planning, experimental design, conducting experiments, analysis and manuscript writing.

Gerstein, Aleeza C: Co-supervisor: Provided guidance in experimental evolution, using compute Canada resources for genomic analysis, statistical analysis, and manuscript writing.

# Table of Contents

# List of Figures

# List of Tables

# List of Abbreviations

| | |
|---|---|
| AMR | Antimicrobial resistance |
| CMB | Combined (prothioconazole & tebuconazole in equal concentration) |
| DON | Deoxynivalenol |
| DMS | DMSO |
| FHB | Fusarium head blight |
| LTEE | Long term evolution experiment |
| MIC | Minimum inhibitory concentration |
| PTZ | Prothioconazole |
| SUMO | Small ubiquitin-like modifier |
| TBF | Tebuconazole |

# Chapter 1

## Introduction

### 1.1 Fusarium graminearum

*Fusarium graminearum* is an ascomycete fungus possessing the unique cell types including hyphae and spores, and unique tissues types including hyphae, perithecia, and sporodochia. *F. graminearum* is haploid, has 4 chromosomes and has a genome that is approximately 35 million base pairs (Cuomo et al., 2007). *Fusarium graminearum* exhibits a life cycle that includes the ability to reproduce both sexually and asexually. The asexual reproductive cycle involves the production of macroconidia that are borne off of sporodochia (Geng et al., 2014). Macroconidia are banana shaped, multicellular structures characterized by a hard protective outer layer, making dispersal by wind less likely due to their weight, and not being forcibly ejected like ascospores (Beyer et al., 2004). Macroconidia can be dispersed by rain or insects. With their protective outer layer, they can easily over winter in the soil and plant debris, and germinate in the spring when conditions are ideal (Beyer et al., 2004).

The sexual reproductive cycle of *F. graminearum* begins with the development of perithecia, which release ascospores (Trail, 2009). It is thought that ascospores are the primary inoculum for infections, as they are forcibly discharged and can travel through the air, landing on spikelets (Sandra et al., 2005). Once the ascospores land on plant tissue, they begin growth with the elongation of the germ tube, then invasive hyphae penetrate into the grain's inner tissues causing damage and producing mycotoxins (Sandra et al., 2005).

### 1.2 Fusarium graminearum in agriculture

*Fusarium graminearum* causes fusarium head blight (FHB), a destructive fungal disease that has been impacting global agriculture for well over a century. The disease was first described in Russia in 1882, where it was linked to the poisoning of humans and animals who consumed the grain, a condition they deemed as "drunken bread" (Gagkaeva et al., 2021). Shortly after, in 1884, it was formally identified in England as "wheat scab" (Smith, 2022).

While FHB has a large history of causing epidemics worldwide, it has become a major threat to North American small cereal grains production in the late 20th and early 21st centuries (*Fusarium Head Blight of Wheat and Barley*, 2003).

### 1.3 Management of fusarium head blight

Management strategies to control FHB infections include the use of resistant crop varieties, crop rotation, and removing crop residue from the previous season (A.-H. Chen et al., 2022). Resistant cultivars have become a cost effective way to combat the infection, but may come with trade offs such as yield reduction (A.-H. Chen et al., 2022; H. W. Schroeder, 1964). Furthermore, no completely FHB-resistant genotypes have been identified in any of the cereal crops. *Fusarium graminearum* has specific host plants including small grain cereals, and removing those hosts for a period of time can cause a decline in the *F. graminearum* population size. For example, by alternating with a non-host plant species on particular fields across growing seasons, the amount of *F. graminearum* inoculum can be reduced. To reduce the amount of *F. graminearum* inoculum in fields, it is good practice to remove crop debris after an infected season (Leplat et al., 2013). This can be accomplished through various methods such as discing, bailing, or cutting the crop shorter, as the fungus overwinters in the residue and serves as a source of inoculum in the spring (Leplat et al., 2013). Another, newer way to combat FHB is with chemical fungicides that were first introduced into agriculture in the 1970s (Price et al., 2015). The development of fungicides became important in managing FHB in Canada and across the world. Triazole fungicides emerged as effective chemical control options, specifically when used with the proper timing.

### 1.4 Azole fungicides

Azoles represent one of the most prominent and widely used classes of antifungal agents, playing a role in clinical management of human fungal infections. Azoles are a class of compounds characterized by a five membered ring containing a nitrogen and an additional non-carbon element, and can be divided into two groups, triazoles and imidazoles. Azoles were first introduced in 1958 in the clinic as a topical cream, followed by the use of azoles in agriculture in the 1970s (Price et al., 2015). Azole fungicides work by inhibiting the 14α demethylase enzyme which is encoded by the *cyp51* gene (Ziogas & Malandrakis, 2015).

### 1.5 Prothioconazole and tebuconazole

Structurally, tebuconazole and prothioconazole share a 1, 2, 4 triazole ring (Figure 1.1A & B). However, on the triazole ring, prothioconazole contains a thione group (C=S), which is unique to this azole. This substitution has profound implications for how the fungicide interacts with its fungal target. Prothioconazole does not inhibit Cyp51, instead, prothioconazole is converted into its active form in the fungal cell of prothioconazole-desthio (Figure 1C) which inhibits Cyp51 (Parker et al., 2013).

Tebuconazole was one of the earlier azole fungicides to gain widespread use in agriculture, emerging on the market in 1989 (McInnes et al., 2023). In Canada, it is a primary component of fungicide products such as Prosaro PRO, by Bayer CropScience where it is combined with other active ingredients, including prothioconazole. Prothioconazole is a more recent fungicide, first introduced in 2004 by Bayer CropScience, and was registered and marketed in the United States and Canada in 2007 (Edwards & Godley, 2010). Prothioconazole is sold solely in products like Proline by Bayer CropScience, or in combination with tebuconazole in products such as TilMOR, also by Bayer CropScience.

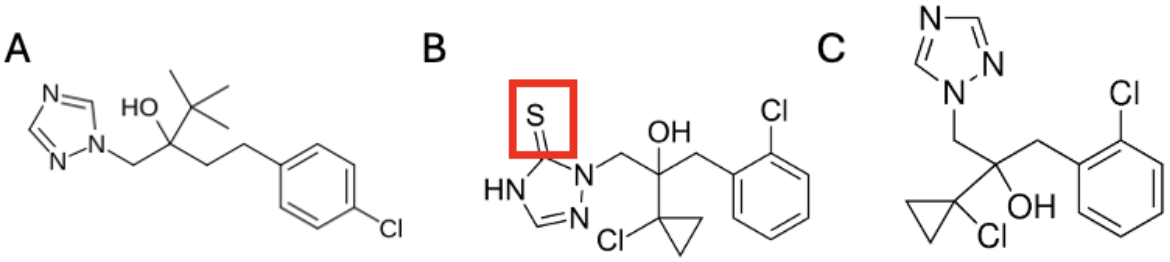


**Figure 1.1 The chemical structures of tebuconazole (A), prothioconazole (B) and the active form of prothioconazole: prothioconazole-desthio (C). The red box highlights the thione bond.**

### 1.7 Antifungal resistance to azoles

In agriculture, the use of antifungals dates back to the 19th century where the first fungicide consisted of copper sulfate which had multi target site action, making it highly unlikely

to allow for the development of resistance (Klittich, 2008) . However, with the introduction of single target site fungicides such as azoles in the 1970s, the widespread selection pressure on a single target site across agricultural fields has increased the risk of resistance development (K. Hollomon & Brent, 1998). The problem of resistance in agricultural settings is particularly concerning because of the high selection pressure exerted by widespread, large-scale application of fungicides (D. W. Hollomon, 2015).

### 1.8 Fungal genetic plasticity

A key characteristic contributing to the adaptability and evolutionary success of *F. graminearum* is its genetic plasticity. Fungi exhibit genome flexibility, allowing them to rapidly respond to diverse and changing environmental conditions (Castiblanco et al., 2020). This plasticity arises from various mechanisms that generate genetic diversity, including spontaneous mutations during DNA replication and induced mutations triggered by environmental stresses like UV radiation or chemical exposure. At the sequence level, genetic diversity is displayed as point mutations, insertions, and deletions (indels), as well, larger scale genomic changes, such as gene duplications and chromosomal rearrangements, also contribute significantly to fungal evolution and adaptation. These genetic alterations can influence a wide array of traits in *F. graminearum*, including its virulence, host specificity, mycotoxin production, fungicide sensitivity, and overall fitness in agricultural ecosystems (Miedaner et al., 2008). Another source of genetic diversity is from recombination during sexual reproduction in *F. graminearum*. Even though asexual reproduction is less costly (Kobayashi, 2019), sexual reproduction provides more genetic diversity through the shuffling of genes, and incorporation of new genetic material from variation within the population (Miedaner et al., 2008).

### 1.9 Laboratory directed evolution

Experimental evolution is a powerful method for studying the process of adaptation in real time. It involves propagating microbial populations in a controlled laboratory setting over many generations to observe how they evolve under specific selective pressures. This approach allows researchers to directly test hypotheses about evolutionary dynamics, such as the rate of adaptation, the role of chance in genetic recombination, and the genetic basis of new traits.

A common approach to experimental evolution in *E. coli* and yeasts is to grow large populations in liquid culture. This method is effective because these organisms have short generation times, allowing for a high number of generations to be studied over a relatively short period. The most famous example is Richard Lenski's long term evolution experiment (LTEE), which began in 1988 with 12 populations of *E. coli* (Lenski, 2003). These populations have been maintained in a simple, glucose-limited medium with daily transfers to fresh media (Lenski, 2017). A constant well defined selective pressure drove the population to improve the *E. coli*'s glucose utilization. By freezing samples of the populations at regular intervals, researchers can later revive ancestral and evolved strains to compare their fitness and analyze the genetic changes that have accumulated over time. On August 7, 2024, the LTEE reached the milestone of running for 35 years and 80,000 generations, providing incredible insight into evolutionary change (Barrick, 2025).

While liquid culture methods work well for experimental evolution experiments with single celled organisms, there are challenges for filamentous fungi due to their multicellular growth. Filamentous fungi such as *Fusarium* or *Aspergillus* grow as a network of hyphae, rather than as free living cells, making it difficult to maintain a well-mixed, uniform population in a liquid culture and to transfer a consistent number of individuals for each new generation. To overcome this, researchers like Schoustra, and his group adapted the experimental evolution methodology. They focused on growing the fungi on solid agar plates. In their study conducted in 2006 on *Aspergilus nudulans*, they maintained populations by transferring a small piece of mycelium from the edge of a growing colony to a new plate every few days (Schoustra et al., 2006). This method, while more labor intensive, mimics the spatial dynamics of fungal growth and allows for the selection of traits related to faster growth or more efficient resource acquisition on a surface.

The power of experimental evolution is its ability to directly observe and replicate evolutionary processes. Unlike historical reconstruction, which relies on fossil records and comparative genomics, this methodology provides a direct link between environmental pressures and phenotypic changes. This allows researchers to test and refine theories about mutation rates, natural selection, and the predictability of evolution. Research in this field has resulted in knowledge in the areas of preadaptation, the role of epistasis, and the evolution of metabolic

functions, such as the ability of one of the LTEE populations to adapt to low glucose environments (Lenski, 2017).

The thesis aims to use the laboratory experimental evolution methodology to test the hypothesis that the selective pressure of tebuconazole, prothioconazole or both fungicides in equal concentration would drive genetic alterations, such as point mutations or larger genomic changes, leading to the evolution of antifungal resistance. By comparing the fungicide sensitivity, and genetics of the evolved strains to the ancestral, we can learn about the ways in which *F. graminearum* evolves to selective pressures that we are using in agriculture. Further, freezing samples at frequent time points during the experiment allows for the later analysis of the specific genetic changes responsible for the observed increases in fungicide tolerance.

# Chapter 2 - Beyond *cyp51*: A novel reduced spore dormancy pathway confers azole resistance in *Fusarium graminearum*


## Abstract:

*Fusarium graminearum* is a major pathogen of wheat and barley, causing annual global agricultural losses exceeding one billion dollars. Historically azole fungicides (demethylation inhibitors) have effectively managed *F. graminearum* infections in Canada, but recent data suggests increasing resistance in populations. Azoles inhibit ergosterol biosynthesis by binding to the active site of Cyp51. Resistance to azoles is often driven by mutations in the *cyp51* gene that alter the enzyme binding site, lowering azole binding affinity. In this study, *F. graminearum* strain DAOMC 233423 was exposed to increasing concentrations of tebuconazole, prothioconazole, a combination of both fungicides, or a solvent carrier control (four replicates each) until strain extinction in the fungicide treatments. All evolved strains exceeded the initial MIC (minimum inhibitory concentration) by 2×-5.1× but only one strain, TBF1, maintained its reduced sensitivity to azoles after long term storage in the freezer. All evolved strains retained a normal growth rate, and were able to successfully infect a fusarium head blight-susceptible wheat cultivar. Strain TBF1, evolved to tebuconazole, retained stable tebuconazole resistance, which was accompanied by impaired spore production. Whole genome sequencing analyses identified a single base insertion in the *smt3* gene in TBF1, resulting in a premature stop codon. The *smt3* gene deletion strains phenocopied the TBF1 strain, with decreased tebuconazole sensitivity and altered macroconidia germination behaviour. Surprisingly, no mutations were identified in any *cyp51* genes.

# Introduction

*Fusarium graminearum* is a devastating fungal pathogen that causes fusarium head blight disease on important small grain cereal crops like wheat and barley across the world (Shishatskaya et al., 2018). Economic losses due to *F. graminearum* infections worldwide have averaged over a billion dollars annually in recent years (Powell & Vujanovic, 2021). These losses include both yield reductions due to shrunken and aborted kernels, and costs associated with the presence of mycotoxins, fungal secondary metabolites that pose safety hazards in food and feed products (Powell & Vujanovic, 2021).

Fusarium head blight is most effectively managed through integrated strategies that combine methods such as crop rotation, residue management, the use of crop cultivars that carry genetic resistance toward the disease, and chemical fungicides (Jørgensen & Heick, 2021). Fungicides provide the most effective and economical control when their use is timed with crop phenology and with environmental conditions that favour pathogen establishment (Abou Ammar et al., 2013). There are multiple classes of fungicides available to manage *F. graminearum*, including azoles, phenylamides, anilino-pyrimidines, quinone outside inhibitors and carboxylic acid amides. Among the available fungicides, those based on azole compounds are preferred for their broad range activity and relatively low cost (Price et al., 2015). Azoles are classified as demethylation inhibitors (DMI) and are part of the Fungicide Resistance Action Committee (FRAC) Group 3 (FRAC, 2025a). Knowledge of the mechanisms of action of the fungicides used on a given farm over time is vital to minimize the risk of fungicide resistance development (FRAC, 2025b).

Azoles target the lanosterol 14α-demethylase enzyme (Cyp51), which is part of the pathway that synthesizes ergosterol, a critical component of the fungal cell membrane (Ziogas & Malandrakis, 2015). By inhibiting the lanosterol 14α-demethylase enzyme, azoles cause an accumulation of the enzyme ligand, methylated lanosterol, which changes the sterol composition of the cell membrane. The altered membrane composition pauses or slows cell growth, with fungicidal effects at sufficiently high concentrations (Jørgensen & Heick, 2021; Taxvig et al., 2008). The various active ingredients that are available across different azole-based fungicides interact with lanosterol 14α-demethylase in slightly different ways. For example, tebuconazole, epoxiconazole, and triadimenol directly attach to the heme iron of cytochrome P450, inhibiting the binding of an $O_2$ molecule to the lanosterol C14-methyl group (Parker et al., 2011; Ziogas &

Malandrakis, 2015). In contrast, prothioconazole does not directly attach to the heme iron of cytochrome P450, and has an alternate method of inhibiting the action of lanosterol 14α-demethylase (Parker et al., 2011). Differences in the precise chemical interaction between various azole compounds and their cellular target suggest that there may be different opportunities for mutations to enhance resistance across different fungicides.

The development of azole resistance within pathogen populations is a concern. Environmental azole exposure is increasing; in the United States, azole use increased 434 % between 2006 to 2016 (Toda et al., 2021). Azoles are systemic and target site specific, two traits that both increase the risk of resistance evolution. Systemic fungicides are transmitted throughout the plant, increasing the proportion of the fungal cell population that is exposed to selection pressure, while a site specific mode of action means that there are likely to be mutations of large effect size to circumvent the mode of action.

The inhibitory effect of azole compounds can be alleviated by mutations in the coding sequence or promoter region of the *cyp51* gene. The number of homologs of the *cyp51* gene vary among fungal species; fungi such as *Candida albicans* (Zhou et al., 2018) and *Cryptococcus neoformans* (Chunquan et al., 2009) have a single *cyp51* gene (also known as *Erg11*), while *Aspergillus fumigatus* (E. Mellado, T. M. Diaz-Guerra, M. Cuenca-Estrella, J. L. Rodriguez-Tudela, 2001) has both *cyp51A* and *cyp51B* genes, and *F. graminearum* has *cyp51A, cyp51B* and *cyp51C* genes (Fan et al., 2013). In *F. graminearum*, *cyp51B* encodes the primary sterol 14α-demethylase, and is also essential for ascospore formation (Fan et al., 2013). The *cyp51B* gene is the most conserved *cyp51* gene across all fungi (Fan et al., 2013). The *cyp51A* gene encodes additional sterol 14α-demethylase and has been characterized as the gene responsible for the fungus's azole sensitivity (Fan et al., 2013). The *cyp51C* gene is unique to the *Fusarium* species, and does not function as a sterol 14α-demethylase, instead it is specifically required for full virulence on wheat, and is linked to the production of the deoxynivalenol (DON) (Fan et al., 2013).

Recently, a comprehensive curation of reported antifungal resistance mutations assessed over 500 publications related to antimicrobial resistance (AMR) among fungi, across 208 anti-fungal compounds (Bédard et al., 2025). For *F. graminearum*, relatively few mutations related to AMR have been identified. Resistance to tebuconazole is conferred by D243N or G443S mutations in *cyp51A*, or by Y137H or S169Y mutations in *cyp51B* (J. Chen et al., 2021; Qian et

al., 2018). Resistance to metconazole is conferred by D243N, G443S or E103Q + V157L mutations in the *cyp51A* gene (Duan et al., 2018). Resistance to thiabendazole is conferred by the H6N mutation in the $\beta_2$-tubulin gene (Sevastos et al., 2016). For *F. graminearum*, as for all fungal species that have been studied for resistance towards azoles, the most common mutations that have been reported fall within or influence the expression of the *cyp51* gene, or influence the intracellular concentration of azoles (Bédard et al., 2025; Price et al., 2015). Changes in the promoter regions of the *cyp51* genes can influence the amount of mRNA, thus, increasing the levels of transcription as a way to combat the cellular toxicity of the azoles (Price et al., 2015).

Antimicrobial resistance is most problematic if resistant mutants retain normal or even improved fitness in the absence of drug (K. Hollomon & Brent, 1998), i.e., if resistance-conferring mutations do not carry associated fitness costs that would hinder resistant strains from increasing in frequency. Beyond the potential to lose critical management tools for protecting agricultural productivity, development of resistance toward fungicides due to environmental azole exposure also raises concerns about cross-over resistance toward the structurally similar azole drugs that are used to treat human fungal infections. For example, the widespread use of azole fungicides in agriculture has directly contributed to the development of *Aspergillus fumigatus* strains that are resistant to the first-line azole treatments for invasive aspergillosis. This makes these infections much harder to treat, and leads to poorer patient outcomes (Berger et al., 2017; Lockhart et al., 2023). Agricultural drug formulations often include multiple components in an effort to decrease the propensity for resistance evolution by requiring mutations to multiple targets.

Deepening our understanding of the pathways towards the evolution of fungicide resistance is critical for maintaining the efficacy of agricultural fungicides. One approach has been to identify mutations in the least sensitive individuals within a wild population. However, this approach is complicated by the unknown history and variable genetic background of strains collected from the wild (Becher et al., 2010). Experimental laboratory evolution is a complementary strategy that has the advantages of knowing the starting population, and of having the ability to precisely manipulate the environment to focus on one specific selective pressure while holding other factors (such as temperature and nutrient availability) constant (Cooper, 2018). Experimental evolution is a powerful system for studying the genetic basis of adaptation and evolution (LaCroix et al., 2017), particularly when paired with whole-genome

DNA sequencing that does not require *a priori* assumptions about where beneficial mutations are likely to arise (e.g., re-sequencing only *cyp51* genes). Somewhat surprisingly, however, this powerful strategy has not been well exploited to understand resistance evolution in agricultural fungal pathogens (Bédard et al., 2025; Price et al., 2015).

To identify mutations that confer decreased sensitivity to azoles in *F. graminearum,* we performed a laboratory evolution experiment where replicate populations founded from the ancestral strain DAOMC 233423 were exposed to increasing concentrations of prothioconazole, tebuconazole, or a combination of both azoles over time. We expected that the different drug treatments might select for different point mutations within the *cyp51* genes, and that mutations to overcome a combination of azoles would arise less frequently. The evolved lineages were genotyped by whole genome sequencing and we compared ancestral and evolved populations for growth rate, sexual and asexual reproductive ability, aggressiveness in causing fusarium head blight on wheat, and cross-resistance to agricultural and clinical azoles.

# Methods

### Laboratory evolution experiment

Replicate lineages of *Fusarium graminearum* strain DAOMC 233423 (synonym Z3639) (Bowden & Leslie, 1999) were evolved on V8 agar in a series of Petri plate transfers under 4 different treatment conditions: a no-drug control (DMS) which was exposed only to the DMSO solvent carrier that was used in the other treatments, tebuconazole (TBF), prothioconazole (PTZ), and tebuconazole + prothioconazole combined (CMB).

Through preliminary experiments that tested different *in vitro* growing conditions, growth conditions were set as V8 agar (per L: 200 mL V8 juice, 0.3 g yeast extract, 3.0 g calcium carbonate) at 28 °C in the dark. The minimum inhibitory concentration (MIC) for TBF, PTZ, and TBF + PTZ (equal concentrations of each compound) was determined based on colony growth on V8 agar beginning from 1,000 macroconidia incubated for 72 hours. The initial MIC for each of the drug treatments was determined to be 10 µM for tebuconazole, 0.8 µM for prothioconazole, and 0.64 µM tebuconazole + 0.64 µM prothioconazole for the combined treatment. To enable successful growth, the initial concentrations at the commencement of the evolution experiment were set below the MICs, at a concentration that reduced colony area by 25 %: 0.8 µM for tebuconazole, 0.2 µM for prothioconazole, and 0.02 µM for each of the drugs in the combined treatment. Stock solutions of each azole compound were prepared in DMSO, and the DMS treatment (control) received an equivalent DMSO exposure.

The ancestral strain was used to establish replicate lineages under each selection regime (n = 4 per treatment), by spotting 10,000 macroconidia (concentration determined by hemocytometer) at the centre of each plate. After 5 days, plates were photographed to capture the colony area, and then the culture was transferred to a new dish via a punch collected from the leading edge of growth, using the back end of a 1 mL pipette tip. For the 5$^{th}$ transfer at a given drug concentration (i.e., after 25 days of continuous growth at the same concentration), a plug from leading edge of growth was transferred into carboxymethyl cellulose broth (CMC; per L: 15 g medium viscosity carboxymethylcellulose sodium salt, 1 g $NH_4NO_3$, 1 g $KH_2PO_4$, 0.5 g $MgSO_4 \cdot 7H_2O$, 1 g yeast extract) to produce macroconidia (asexual spores) for preservation (-80 °C, in 30 % sterile glycerol) as living record along the evolutionary path of each lineage.

The azole concentration was doubled every 25 days; at each step increase, 10,000 macroconidia were spotted in the centre of each Petri dish. The process of doubling the azole concentration every 25 days continued until there was no visible growth after 5 days of incubation. For lineages that went extinct, further characterizations were based on the end point of the previous azole concentration (i.e., the final preservation stock in the series).

**Acquired resistance stability**

After storage in the freezer longer than 30 days, final evolved strains were revived onto azole-free V8 agar. The strains were incubated at 28 ℃ for 72 hours, then a loop of mycelium was transferred into 30 mL of CMC broth in a 125 mL conical flask and shaken at 200 rpm at 28 ℃ for 72 hours. The inoculated broth was strained through a 40 µm cell strainer into a centrifuge tube. The macroconidia were spun down, supernatant drained, and re-suspended in sterile water. The concentration of macroconidia was counted using a hemocytometer and these macroconidia were used to assess resistance toward azoles.

**Phenotyping of evolved strains**

Growth rate was assessed as colony diameter on a drug-free medium. To ensure an equal readiness to grow in all tests, a suspension of macroconidia was spotted onto drug-free V8 agar, allowed to grow for 4 days, and then a plug from the leading edge of growth was transferred onto another drug-free plate for growth rate assessment. Photographs were taken at 24, 48 and 72 hours, and colony surface area ($cm^2$) was calculated in ImageJ, setting the scale for each image by the diameter of the Petri dish. Measurements were taken from 3 biological replicates. The resulting growth area values were then subjected to an Analysis of Variance (ANOVA) to statistically compare each strain.

Aggressiveness as pathogens causing fusarium head blight (FHB) was assessed with an *in planta* greenhouse experiment. Potting mix was prepared by combining 100 g of fertilizer (Osmocote 14-14-14) per 20 L of potting mix (Sungro Sunshine Mix). Pots (4 L) were lined with a double layer of paper towel and filled to 5 cm from the top with the prepared soil mixture, lightly compacted. An FHB-susceptible cultivar of wheat, CDC Teal, was planted with four seeds per pot. Additional slow-release fertilizer (13-12-12 ACER NT 3-4 month + micros; 18 g per pot) was spread on top of each pot. Pots were thinned to 3 plants if all 4 seeds emerged, and

were culled from the experiment if fewer than 3 plants emerged. Pots were watered when the soil appeared dry. Additional fertilizer (20-20-20 Peters Professional, 125 mg in 500 mL per pot) was provided every 14 days until spike formation, at which point fertilization was discontinued.

Pots were arranged in a greenhouse in 10 blocks of 7 pots each, with 3 plants in each pot; the plant was considered to be the experimental unit. Each block of 21 plants included, in randomized order, one plant inoculated with each of the sixteen evolved strains, four plants inoculated with the ancestral strain, and one mock-inoculated control plant. Each evolved strain was thus inoculated onto 10 wheat heads. Macroconidia were prepared for each of the strains in CMC broth as described above, but resuspended in sterile water at a concentration of 1,000 macroconidia per 10 µL. After at least one wheat head on each plant began flowering, the middle spikelet of a flowering head was marked with ink, and 10 µL of the appropriate inoculant was pipetted into a floret. Inoculated heads were sprayed with water and covered with a plastic bag to maintain a humid environment conducive for infection. The plastic bags were removed after 48 hours. Before counting visual symptoms on day 4 post inoculation, 18 plants (6 pots) were culled during the experiment due to the appearance of non-fusarium head blight disease symptoms. The number of visually symptomatic (bleached) spikelets was recorded 4, 7, and 10 days post-inoculation. The Area Under the Disease Progress Curve (AUDPC) was calculated for each plant using the trapezoidal method (R package “agricolae”, (Mendiburu, 2023)). This procedure integrates disease severity counts over time into a single value, summarizing the total disease over the observation period. The resulting AUDPC values were then subjected to an Analysis of Variance (ANOVA) (comparison of AUDPC ~ inoculant) to statistically compare the effects of different treatments on disease development.

To assess reproductive capacity, we counted macroconidia, observed the morphology of macroconidia, and tested the ability to produce perithecia through homothallic sexual reproduction. Macroconidia from the frozen preservation stocks were plated onto V8 agar and incubated for 72 hrs before a mycelial plug was transferred from the leading edge of growth, into CMC broth (30 mL broth in a 125 mL baffled conical flask) and shaken at 300 rpm. After 72 hrs, each culture was strained through a 40 µm cell strainer and the macroconidia in the filtrate were counted using a hemocytometer. Three biological replicates were analyzed. The resulting macroconidia counts were then subjected to an Analysis of Variance (ANOVA) with Tukey post-hoc contrasts to statistically compare the different strains. Morphology of macroconidia was

observed by microscopy (Evos Cell Imaging System, ThermoFisher Scientific). Production of perithecia was assessed on carrot agar (boil 100 g of fresh organic carrots for 10 minutes in 250 mL of water, blend until smooth, add 5 g of agar); each plate was inoculated at the centre and incubated in the dark for 6 days, at which point the mycelium was flattened and removed with 1 mL filter-sterilized 2.5 % Tween 60 and a stick spreader. The plates were placed under 24 hr fluorescent light for 10 days, repeating the scraping whenever mycelium appeared to grow. Perithecia were examined using a dissecting microscope.

**Genotyping of evolved strains**

We performed short-read whole-genome sequencing to genotype the evolved strains. Mycelium was harvested from deep Petri plate cultures on V8 agar, lyophilized, and ground to a powder (30 sec, 3.1 m/s; OMNI International Bead Ruptor Elite). DNA was extracted using the DNeasy Plant Pro kit (Qiagen), followed by additional purification (Clean and Concentrate kit, ZYMO Research). DNA quality and concentration were quantified spectrophotometrically (NanoDrop One, Thermo Scientific). The concentration of DNA in each sample was normalized to 25 μg/μL and extracts were sent to SeqCoast Genomics (Portsmouth, USA) for library preparation (DNA Prep tagmentation kit with unique dual indexes, Illumina) and sequencing (NexSeq2000 with 2×150 bp paired reads, Illumina). DRAGEN v4.2.7 was used to assess read quality, demultiplex and trim adapter sequences.

The sequence reads were processed with Trimmomatic v0.39 to remove low-quality bases from the leading and trailing ends of each read, with the default parameters (*USADELLAB.org - Trimmomatic: A Flexible Read Trimming Tool for Illumina NGS Data*, n.d.). Quality scores were assessed with FASTQC v0.12.1 and MultiQC v1.13 to ensure the trimming process had successfully improved the data quality (*Babraham Bioinformatics - FastQC A Quality Control Tool for High Throughput Sequence Data*, n.d.). The reference genome (Z3639 v4.0) accessed from Mycocosm was indexed using bwa v0.7.17 with the bwtsw algorithm, and alignment of the trimmed reads to the reference was computed with bwa-mem (*Babraham Bioinformatics - FastQC A Quality Control Tool for High Throughput Sequence Data*, n.d.; Li H And Durbin, 2009). The alignment of the trimmed reads was sorted by genomic coordinates using Picard Tools v2.27.4 SortSam, then the alignment quality was checked using Picard Tools CollectAlignmentSummaryMetrics (Broad Institute, 2019). The SAM files were

converted to Binary Alignment Map (BAM) files using Picard Tools SamFormatConverter for more efficient computing use (Broad Institute, 2020). Picard Tools MarkDuplicates and FixMateInformation were used to identify and remove duplicate reads, and to fix mate pairs (Broad Institute, 2024). A sequence dictionary of the reference was created with gatk v4.4.0.0 CreateSequenceDictionary (*CreateSequenceDictionary (Picard)*, 2019), then the reference was indexed using SamTools v1.20 faidx (H. Li et al., 2025). Variants were called using the default parameters of Genome Analysis Toolkit tool Mutect2 (Benjamin et al., 2019). The input files for Mutect2 were the reference genome sequence (DAOMC 233423), the ancestral strain (ANC) as the matched normal, and the evolved strains as the mutants. Each evolved strain was run individually. Variants of interest were those that scored with a "PASS," which indicates high-likelihood somatic mutation that clears statistical hurdles designed to remove sequencing and alignment artifacts as well as germline variants (*Mutect2*, 2025). Variants were annotated with snpEff using a custom-built database from annotation files available at Mycocosm for *F. graminearum* (*Home - Fusarium Graminearum Z3639 v4.0*, n.d.). SnpEff determined if the mutations were in a gene, or close to a gene. CLC Genomics Workbench (Qiagen) was used to visualize read alignments to the reference sequence to confirm the absence of mutations in the *cyp51* genes. The average depth coverage was 87× with minimum coverage of 60× and maximum coverage of 105×.

**Gene knockout using CRISPR-Cas9**

We used CRISPR-Cas9 gene editing to validate one mutation of interest, following the protocols of (Sharma et al., 2022). Macroconidia (1 mL at $2\times10^6$ macroconidia/mL) were inoculated in 50 mL of oxgall media (per L: 10 g peptone, 10 g glucose, 15 g oxgall), and shaken at 200 rpm at 22 ℃ for 18 hours, until germ tubes were 2-3 times the length of the macroconidium. The germinated macroconidia were trapped on a 0.45 μm mesh cell strainer, washed with 1.2 M KCl, and incubated in an enzyme cocktail (500 mg yatalase, 200 mg driselase, 200 mg lysing enzyme in 20 mL of 1.2 M KCl, filter sterilized) at 28 ℃ and 100 rpm. When approximately 70% of the germlings had been converted into protoplasts, protoplasts were filtered through a 40 μm cell strainer and pelleted with gentle centrifugation (3500 rpm, 5 min).

Protoplasts were washed three times with 25 mL 1.2 M KCl and resuspended at $2\times10^7$ protoplasts / mL in STC buffer with DMSO (per 200 mL: 43.72 g sorbitol, 2 mL 1 M Tris-HCl pH 8, 1.47 g $CaCl_2\cdot2H_2O$, 6 mL DMSO). Aliquots of suspended protoplasts were distributed into 1.5 mL tubes and stored at -80 C.

CRISPR RNAs (crRNA) were designed based on the flanking regions of the *smt3* gene, using CHOPCHOP (Labun et al., 2019) with parameters set for organism = *Fusarium graminearum* and using CRISPR/Cas9 for knock-out. The target site was selected based on a high efficiency score, with GC content between 40-60, and no self complementary regions. The crRNA protospacer (Table 1) was ordered from IDT.

The repair template was designed to replace the *smt3* gene with a hygromycin resistance gene. The 5' Homologous Repair Template (HRT) primer consisted of the 35 base pairs before the start codon of the *smt3* gene, together with the first 35 base pairs of the *hygR* gene. Similarly, the 3' HRT consisted of the end of the *hygR* gene together with sequence from immediately downstream of *smt3*. These primers (Table 1) were ordered as Ultramer DNA Oligos from IDT. *Escherichia coli* DH5α containing the pRF-HU2 plasmid with the hygromycin resistance gene was grown in LB broth for 24 hours. Plasmids were isolated using the Monarch Plasmid Miniprep extraction kit (New England Biolabs). The repair template was assembled by running PCR reactions with the HRT primers and High Fidelity Phusion Master Mix (Thermo), following the recommended PCR conditions. The expected length of the PCR product was confirmed by gel electrophoresis. The PCR product was cleaned using the PureLink PCR Purification kit (Invitrogen), concentration was determined spectrophotometrically (NanoDrop One, ThermoFisher Scientific). The Cas9-gRNA ribonucleoprotein (RNP) complex was assembled in vitro before being introduced to protoplasts.

Protoplasts were thawed on ice. The RNP complex, protoplasts, 9 µg of repair template and 25 µL of PEG 4000 (per 100 mL: 60 g polyethylene glycol, 45 mL 1 M Tris-HCl, 0.74 g $CaCl_2\cdot2H_2O$), were combined and incubated at room temperature for 20 min. The volume was filled to 2 mL with STC buffer, then 2-3 mL of TB3 media (per L: 3 g yeast extract, 3 g casamino acids, 200 g sucrose) was added and the tube was incubated at 25 ℃ and 150 rpm for 18-20 hours. The next day, 300 µL of regenerated protoplast suspension was mixed with 20 mL of fresh molten TB3 containing 0.7% low melting point agarose and 0.1 mg/mL hygromycin B.

The media was poured into sterile Petri plates and incubated at 28 ℃ for 5-6 days until the appearance of resistant colonies.

To confirm that the intended edit occurred, qPCR was used. Mycelium of ANC, TBF1, *Δsmt3_1* and *Δsmt3_2* strains was harvested from deep Petri plate cultures on V8 agar, lyophilized, and ground to a powder (30 sec, 3.1 m/s; OMNI International Bead Ruptor Elite). DNA was extracted using the DNeasy Plant Pro kit (Qiagen), followed by additional purification (Clean and Concentrate kit, ZYMO Research). DNA quality and concentration were quantified spectrophotometrically (NanoDrop One, Thermo Scientific). The concentration of DNA in each sample was normalized to 25 µg/µL. PowerTrack SYBR Green Real-Time PCR Master Mix was used for qPCR, targeting three genes of interest: the hygromycin resistance gene, the *smt3* gene, and a reference single-copy gene *tri6*. following the recommended protocol. The qPCR was run with technical duplicates and a thermal cycling program consisting of: 95 ℃ for 15s, cooled to 60 ℃ for 1 minute, plate read, repeated 40 times. In addition to validating the absence of *smt3* and the presence of the hygromycin resistance gene where expected, the copy number of the inserted hygromycin resistance gene was estimating, using the formula: gene copy number = $2^{(ct\_tri6-ct\_hyg)}$.

**Macroconidia imaging**

Macroconidia were produced as described above for the ancestral, TBF1, *Δsmt3_1* and *Δsmt3_2* strains. Macroconidia were strained through a 40 µm cell strainer, and washed twice with 30 mL sterile water and counted with a hemocytometer. Macroconidia were placed in a 96 well plate with approximately 100 macroconidia in each well with 200 µL of sterile water. The plate was incubated at 4 ℃ for 48 hours, then imaged (Evos Cell Imaging System, ThermoFisher Scientific).

# Results

### Experimental laboratory evolution

A total of sixteen replicate lineages were evolved to one of four drug exposure treatments: prothioconazole (PTZ), tebuconazole (TBF), both azoles in equal combination (CMB), and DMSO as a control no-drug treatment (DMS). The initial drug concentration for each treatment was set to the concentration that reduced the 5-day growth area by 25%, when initiated from macroconidia of the ancestral strain. To initiate the experiment, 10,000 macroconidia were spotted in the middle of a V8+ azole treatment plate and incubated. Every five days, a transfer was done by removing a mycelial plug at the leading growth edge and placing it in the middle of a new plate. Every fifth transfer, macroconidia were produced in CMC broth, an aliquot was preserved at -80 °C, and another aliquot was spotted onto a fresh plate containing double the previous drug concentration. The experiment concluded when each lineage either went extinct (complete failure to grow at the next increase in azole concentration), or when 40 transfers were reached (DMS control treatment only). We will refer to the terminal population from each lineage as the "evolved strain".

The four lineages in the drug-free DMS control treatment exhibited consistent and steady growth throughout the experiment, irrespective of whether the inoculum consisted of macroconidia or of mycelium. By contrast, azole-evolved lineages displayed fluctuating growth patterns, with dips in colony area at each increase in azole concentration (Figure 2.1A), which also corresponded to use of macroconidia as inoculum. The four PTZ-exposed lineages went extinct when the drug concentration exceeded four × the ancestral MIC, while CMB-exposed lineages went extinct at 2.5× the ancestral MIC. TBF-evolved lineages were more variable; TBF2 went extinct at 2× the ancestral MIC, while the remaining lineages went extinct at five point one × the ancestral MIC. Overall, the  CMB-exposed lineages went extinct the fastest.

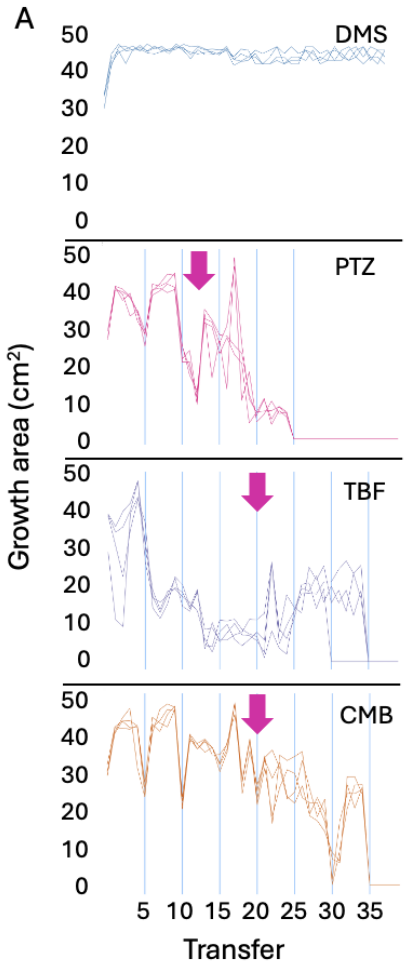


B

| | Treatment & azole concentration (μM) | | |
|---|---|---|---|
| Transfer | PTZ | TBF | CMB |
| 1-5 | 0.2 | 0.8 | 0.02 |
| 6-10 | 0.4 | 1.6 | 0.04 |
| 11-15 | 0.8 | 3.2 | 0.08 |
| 16-20 | 1.6 | 6.4 | 0.16 |
| 21-25 | 3.2 | 12.8 | 0.32 |
| 26-30 | ~~6.4~~ | 25.6 | 0.64 |
| 31-35 | ~~Extinct~~ | 52.2 | 1.28 |
| 36-40 | ~~Extinct~~ | ~~Extinct~~ | ~~Extinct~~ |

C

| | PTZ | TBF1, 3 & 4 | TBF2 | CMB |
|---|---|---|---|---|
| Initial MIC (μM) | 0.8 | 10 | 10 | 0.2 |
| Final evolved concentration (μM) | 3.2 | 51.2 | 25.6 | 1.28 |
| Exceeded initial MIC by | 4× | 5.1× | 2.5× | 2× |

**Figure 2.1 The results summary from the laboratory-directed evolution experiment A. Colony growth area was measured 5 days after each transfer. Every fifth transfer was initiated from macroconidia (vertical bars), other transfers were initiated from a mycelium plug at the leading edge of the growth front. The azole concentration in PTZ, TBF and CMB treatments were doubled at the same time as the macroconidia transfers. Each line indicates one of four independently evolved populations in each treatment group. The arrows indicate the point at which each treatment was exposed to the MIC of the ancestral strain. B. Summary table of the concentrations for each transfer. C. Summary table.**

**Acquired resistance was generally unstable**

The evolved strains were revived from -80 °C freezer stocks and re-evaluated for their ability to grow at their previous maximum azole concentration where successful growth was observed. Surprisingly, only evolved strain, TBF1, was able to grow at the terminal drug concentration when plates were inoculated with macroconidia (Figure 2.2A). By contrast, although all evolved strains and the ancestral strain could grow to some degree on the terminal concentration when inoculated as mycelium, only evolved strains TBF1 and TBF3 outperformed the ancestor (Figure 2.2A). Thus, the majority of evolved strains lost the expected enhanced azole resistance (based on improved growth ability to high azole concentrations at the end of the evolution experiment) after being frozen and revived. To determine at which point in the evolutionary progression the TBF1 lineage acquired enhanced resistance, we revived the intermediate time points. Phenotypes were identical to that of the final evolved strain beginning at 20th transfer, and at all timepoints following (Figure 2.2B).

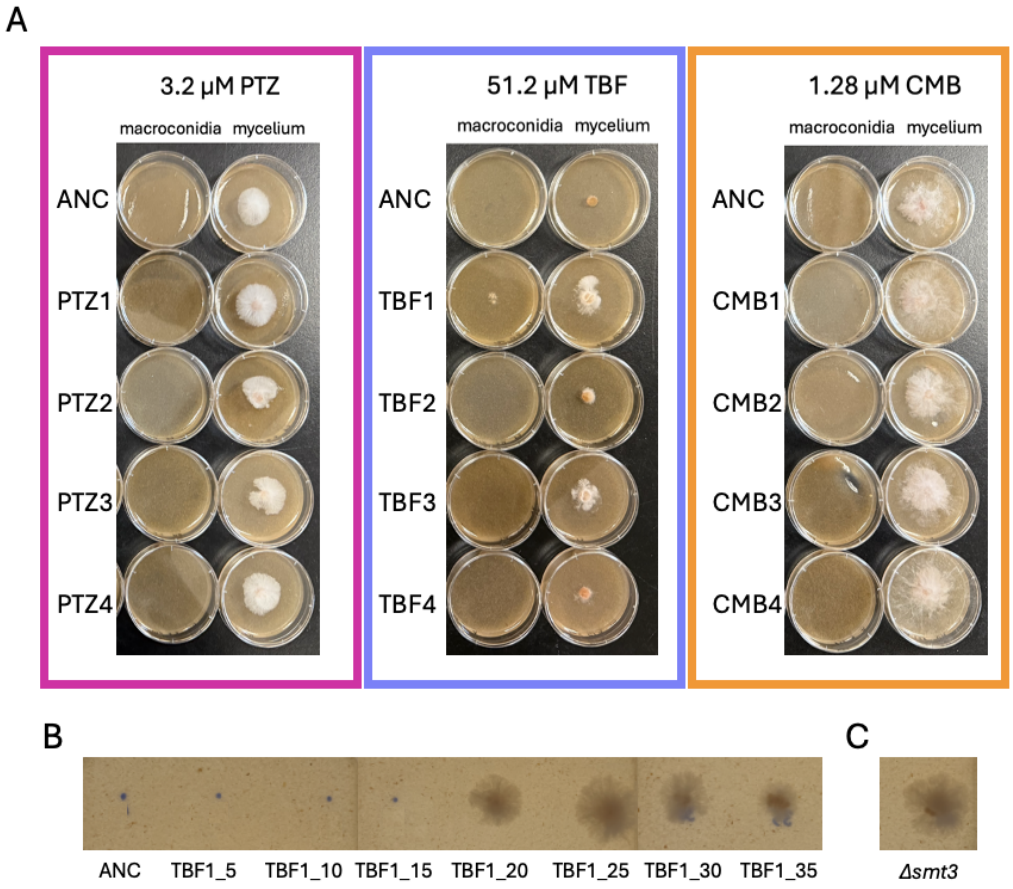


**Figure 2.2 Phenotypic stability of the evolved strains. A. Colony growth of the ancestral and evolved strains, after being revived from storage at -80 °C. The tested concentrations are the maximum concentrations at which growth was achieved during the evolution experiment. Plates were inoculated with either macroconidia or with actively growing mycelium from a plug. B. Each timepoint in the TBF1 lineage was inoculated with approximately 1,000 macroconidia on V8 agar with 20 µM tebuconazole. This image was taken after 4 days of incubation at 28 °C. C. The *Δsmt3_1* strain inoculated with approximately 1000 macroconidia on V8 agar with 20 µM tebuconazole and incubated for 4 days.**

**Evolved strains were generally phenotypically similar to the ancestor**

In the absence of azole exposure, there were no apparent costs due to changes that arose in the evolved lineages. All evolved strains (and the ancestral strain) had the same growth rate on azole-free V8 media when initiated from macroconidia (Figure 2.3A; one-factor ANOVA, $F_{16, 34} = 0.745$, $p = 0.73$). Similarly, in an *in planta* greenhouse disease assay, all evolved strains caused fusarium head blight (scored by diseased spikelets Figure 2.3B) and had a similar level of aggressiveness to a susceptible variety of wheat (Figure 2.3C; ANOVA: $F_{20, 168} = 1.443$, $p = 0.11$). Macroconidia production in the evolved strains was similar to the ancestor with the exception of a significant reduction for TBF1 (Figure 2.4A, 2.4B; ANOVA: $F_{16, 34} = 2.746$, $p = 0.007$). A visual evaluation of the macroconidia indicated that TBF1 produced macroconidia with an altered germination phenotype; in contrast to typical macroconidia that remain dormant under cold, low nutrient conditions, TBF1 produced macroconidia that begin to swell and germinate immediately upon formation (Figure 2.4C).

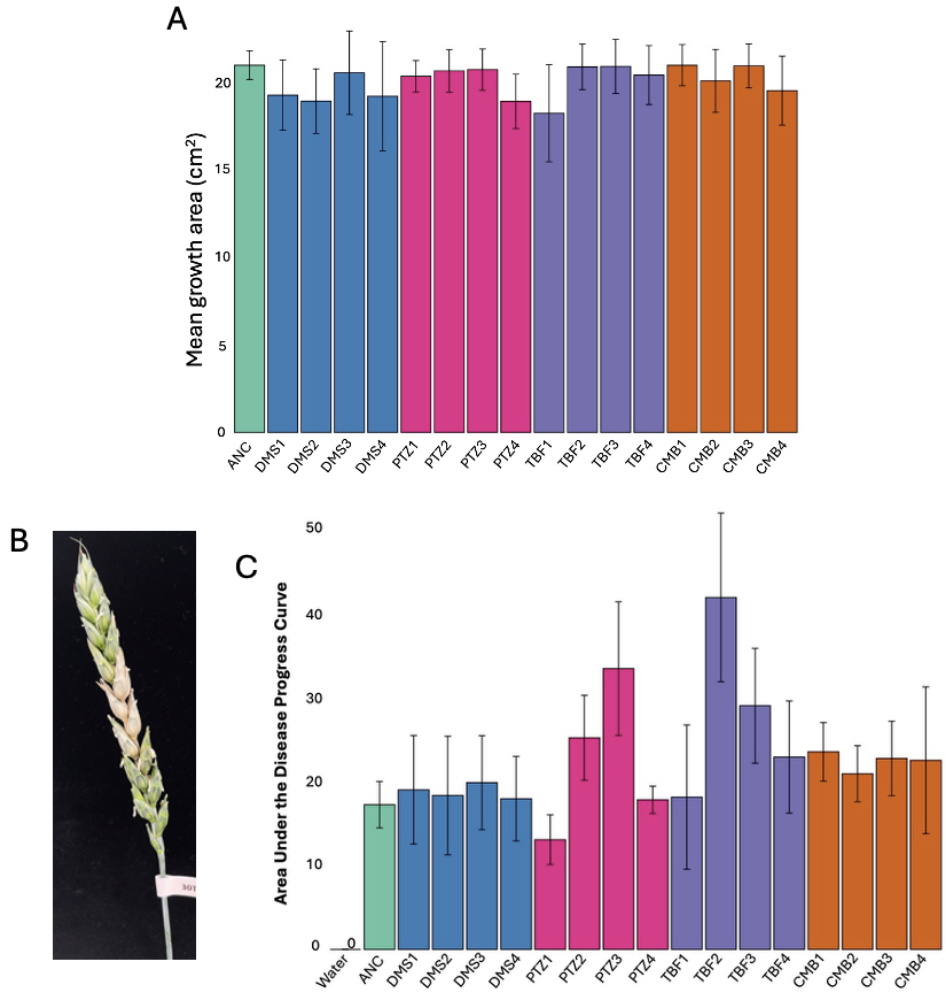


**Figure 2.3** Phenotypic measurements for growth ability and aggressiveness on wheat. **A.** Colony growth area for evolved strains grown on azole-free V8 agar after 72 hours, started from a mycelium plug. Shown are the means ± standard deviation of n = 3 Petri dishes per strain. There were no significant differences among strains (ANOVA, $p = 0.73$). **B.** A typical diseased wheat head from the experiment, showing four symptomatic spikelets. **C.** The area under the disease progress curve, based on counts of symptomatic spikelets at days 4, 7 and 10 post inoculation. The number of plants per treatment ranged from 7-10 for the water control and each evolved lineage, and 36 for the ancestral. The error bars represent the standard deviation. There were no statistically significant differences in AUDPC among evolved strains (ANOVA, $p = 0.11$).

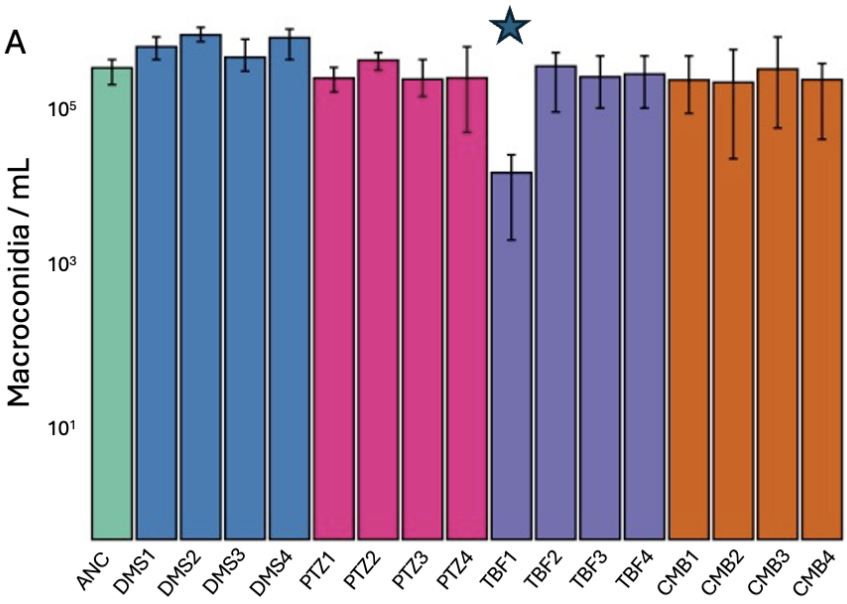


B

| Samples | Diff | P-value |
|---|---|---|
| TBF1-ANC | -1.226 | 0.004 |
| TBF1-CMB1 | -1.041 | 0.028 |
| TBF1-CMB2 | -0.869 | 0.128 |
| TBF1-CMB3 | -1.056 | 0.024 |
| TBF1-CMB4 | -1.001 | 0.04 |
| TBF1-DMS1 | -1.451 | < 0.001 |
| TBF1-DMS2 | -1.583 | < 0.001 |
| TBF1-DMS4 | -1.535 | < 0.001 |
| TBF1-DMS3 | -1.322 | 0.002 |
| TBF1-PTZ1 | -1.12 | 0.013 |
| TBF1-PTZ2 | -1.314 | 0.002 |
| TBF1-PTZ3 | -1.084 | 0.018 |
| TBF1-PTZ4 | -0.982 | 0.048 |
| TBF2-TBF1 | 1.181 | 0.007 |
| TBF3-TBF1 | 1.089 | 0.017 |
| TBF4-TBF1 | 1.12 | 0.013 |

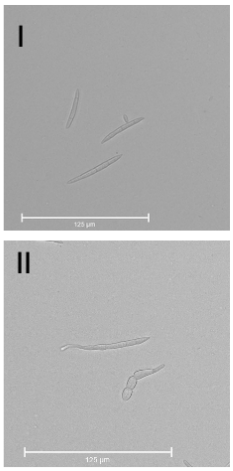


**Figure 2.4** Summary of the macroconidia production ability of evolved strains, highlighting the difference TBF1 compared to all other strains. **A**. Production of macroconidia by the ancestral and evolved strains in CMC broth. The bar height indicates the mean of three replicate flasks per strain, error bars indicate the standard deviation. Macroconidia counts are presented on a $\log_{10}$ scale. The star indicates the strain for which macroconidia production was significantly reduced. **B.** Significantly fewer macroconidia were produced by the evolved strain TBF1 than by all other strains except for CMB2 (ANOVA with Tukey contrasts, $p < 0.05$). **C.** Images of macroconidia from the ancestral strain **(I)** evolved strain TBF1 **(II)**, after 48 hours at 4 °C suspended in sterile water at a concentration of 0.5 macroconidia/µL.

Genotyping of evolved strains

The 16 evolved strains, as well as timepoints along the TBF1 lineage, were Illumina short-read whole genome sequenced. A total of 100 high-confidence genetic variants were identified across all evolved strains, with the number of variants per strain ranging from 1 to 10 (mean 6.25, SD 3.30). All of the evolved strains from the single drug PTZ and TBF treatments had between seven and ten variants, while only a single DMS and none of the CMB strains had more than five variants. The majority of variants were either intergenic (n = 34), upstream or downstream of a gene (n = 29), in the 5' or 3' untranslated region (UTR) of a gene (n = 6), or caused synonymous amino acid changes (n = 12). Only 19 variants were predicted to cause a change in the amino acid sequence of a protein (n = 16 non-synonymous mutations, n = 3 small insertions or deletions) (Figure 2.5, Table S1). Surprisingly, there were no identified mutations in the *cyp51* genes (*cyp51A, cyp51B* or *cyp51C*) in any of the evolved strains. There were not any chromosomal or partial aneuploidies suggested by examining read depth across the genome (Supporting Data Figure S2).

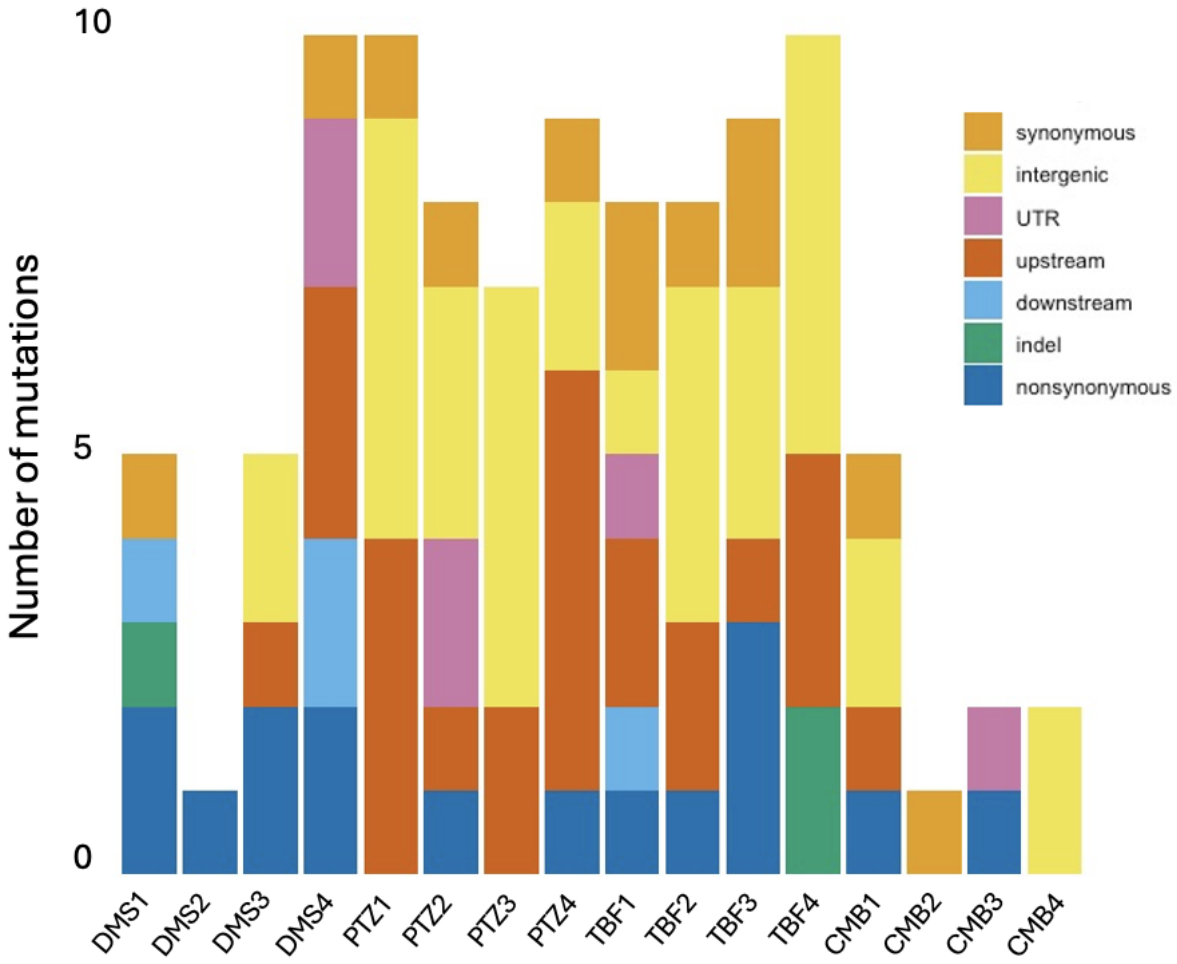


**Figure 2.5 The distribution of high-confidence mutations that were called by Mutect2 in the variant calling pipeline, across all 16 evolved strains from the endpoint of the evolution experiment.**

## Table S1. Mutect2 called variants with annotations

| Strain | Chr | Position | REF | ALT | Annotation | Gene | Amino.Acid | Information | AnnotSimple |
|---|---|---|---|---|---|---|---|---|---|
| **CMB1** | 1 | 1023580 | G | A | synonymous_variant | gene_387 | p.Glu7Glu | NA | synonymous |
| **CMB1** | 2 | 9026875 | T | A | upstream_gene_variant | gene_7412 | NA | NA | upstream |
| **CMB1** | 3 | 5112130 | T | A | intergenic_region | gene_11981-gene_11982 | NA | Complex 1 LYR protein | intergenic |
| **CMB2** | 4 | 6552285 | G | A | synonymous_variant | gene_9732 | p.Ser64Ser | Oxysterol-binding protein, Signal transduction mechanisms , Oxysterol-binding protein | synonymous |
| **CMB4** | 1 | 293115 | G | A | intergenic_region | gene_94-gene_95 | NA | NA | intergenic |
| **DMS1** | 4 | 2595604 | G | A | synonymous_variant | gene_8334 | p.Ala1220Ala | Protein kinase ATM/Tel1, involved in telomere length regulation and DNA repair, Chromatin structure and dynamics , Phosphatidylinositol 3-/4-kinase, catalytic domain | synonymous |
| **DMS4** | 1 | 5396327 | C | A | 5_prime_UTR_variant | gene_1833 | NA | DNA mismatch repair protein - MLH3 family, Replication, recombination and repair , MutL, C-terminal, dimerisation | UTR |
| **DMS4** | 2 | 8344068 | G | A | synonymous_variant | gene_7145 | p.Pro159Pro | Transcription factor, Myb superfamily, Transcription , SANT/Myb domain | synonymous |
| **DMS4** | 2 | 9028661 | G | A | upstream_gene_variant | gene_7412 | NA | NA | upstream |
| **DMS4** | 4 | 3962830 | C | A | upstream_gene_variant | gene_8850 | NA | Auxilin-like protein and related | upstream |

| | | | | | | | | | |
|---|---|---|---|---|---|---|---|---|---|
| | | | | | | | | proteins containing DnaJ domain, General function prediction only , Ubiquitin-associated domain/translation elongation factor EF-Ts, N-terminal | |
| **PTZ1** | 1 | 7343159 | T | A | upstream_gene_variant | gene_2547 | NA | NA | upstream |
| **PTZ1** | 4 | 6957462 | G | A | upstream_gene_variant | gene_9902 | NA | NA | upstream |
| **PTZ2** | 2 | 5846834 | C | A | 5_prime_UTR_variant | gene_6240 | NA | Argininosuccinate lyase, Amino acid transport and metabolism , Fumarate lyase, N-terminal, Argininosuccinate lyase., Urea cycle and metabolism of amino groups | UTR |
| **PTZ2** | 4 | 4900817 | G | A | 5_prime_UTR_premature_start_codon_gain_variant | gene_9177 | NA | Ribosomal protein/NADH dehydrogenase domain | UTR |
| **PTZ2** | 4 | 6957462 | G | A | upstream_gene_variant | gene_9902 | NA | NA | upstream |
| **PTZ3** | 4 | 6957462 | G | A | upstream_gene_variant | gene_9902 | NA | Glycosyl hydrolase, five-bladed beta-propellor domain | upstream |
| **PTZ4** | 2 | 1580845 | T | A | upstream_gene_variant | gene_4680 | NA | NA | upstream |
| **PTZ4** | 2 | 3996443 | G | A | synonymous_variant | gene_5485 | p.Ser345Ser | Cytochrome P450 CYP3/CYP5/CYP6/CYP9 subfamilies, Secondary metabolites biosynthesis, transport and catabolism , Cytochrome P450, Benzoate 4-monooxygenase., Benzoate | synonymous |

| | | | | | | | | | |
|---|---|---|---|---|---|---|---|---|---|
| | | | | | | | | degradation via CoA ligation | |
| **PTZ4** | 4 | 1255611 | G | A | upstream_gene_variant | gene_7877 | NA | Permease, cytosine/purines, uracil, thiamine, allantoin | upstream |
| **PTZ4** | 4 | 6957462 | G | A | upstream_gene_variant | gene_9902 | NA | NA | upstream |
| **TBF1** | 1 | 747350 | C | A | 3_prime_UTR_variant | gene_278 | NA | NA | UTR |
| **TBF1** | 3 | 1602213 | C | A | upstream_gene_variant | gene_10777 | NA | Ribosomal protein S18, Translation, ribosomal structure and biogenesis , Ribosomal protein S13 | upstream |
| **TBF1** | 3 | 3563456 | C | A | synonymous_variant | gene_11421 | NA | Predicted phospholipase, Lipid transport and metabolism , \N | synonymous |
| **TBF3** | 1 | 618727 | C | A | missense_variant | gene_226 | p.Pro22Gln | Glycoside hydrolase, family 16 | nonsynonymous |
| **TBF3** | 2 | 1541178 | C | A | missense_variant | gene_4665 | p.Gly56Cys | Uncharacterized conserved protein, Function unknown , Impact, N-terminal | nonsynonymous |
| **TBF3** | 2 | 2999559 | G | A | upstream_gene_variant | gene_5129 | NA | ATP sulfurylase (sulfate adenylyltransferase), Inorganic ion transport and metabolism , Adenylylsulphate kinase, Sulfate adenylyltransferase., Purine metabolism | upstream |
| **TBF3** | 3 | 4795250 | G | A | synonymous_variant | gene_11877 | p.Arg527Arg | NmrA-like domain | synonymous |
| **TBF3** | 4 | 1984139 | G | A | missense_variant | gene_8127 | p.Ser1457Phe | Uncharacterized conserved coiled-coil protein, Function unknown | nonsynonymous |

| | | | | | | | | | |
|---|---|---|---|---|---|---|---|---|---|
| | | | | | | | | , Tetratricopeptide, MLP1/MLP2-like | |
| **TBF4** | 3 | 5086493 | G | A | intergenic_region | gene_11981-gene_11982 | NA | Complex 1 LYR protein | intergenic |
| **TBF4** | 3 | 5086497 | T | A | intergenic_region | gene_11981-gene_11982 | NA | Complex 1 LYR protein | intergenic |
| **PTZ3** | 3 | 5127061 | TT | AA | intergenic_region | gene_11981-gene_11982 | NA | CHAT domain | intergenic |
| **DMS4** | 4 | 6464655 | CC | AT | missense_variant | gene_9698 | p.Trp274Tyr | Predicted hydrolase (HAD superfamily), General function prediction only , HAD-like domain | nonsynonymous |
| **CMB1** | 3 | 5109716 | T | C | intergenic_region | gene_11981-gene_11982 | NA | Complex 1 LYR protein | intergenic |
| **CMB3** | 3 | 3216317 | T | C | missense_variant | gene_11291 | p.Glu848Gly | TGc (transglutaminase/ protease-like) domain-containing protein involved in cytokinesis, Cell cycle control, cell division, chromosome partitioning , Transglutaminase-like | nonsynonymous |
| **DMS1** | 1 | 2562009 | CAG ATA GTT GAC TAA GAA | C | frameshift_variant | gene_910 | p.Phe3fs | Cutinase, Cutinase., \N | nonsynonymous |
| **DMS4** | 1 | 5396319 | T | C | 5_prime_UTR_variant | gene_1833 | NA | DNA mismatch repair protein - MLH3 family, Replication, recombination and repair , MutL, C-terminal, dimerisation | UTR |
| **PTZ1** | 3 | 6650298 | T | C | upstream_gene_variant | gene_12469 | NA | NA | upstream |
| **PTZ1** | 3 | 6650298 | T | C | upstream_gene_variant | gene_12469 | NA | NA | upstream |

| | | | | | | | | | |
|---|---|---|---|---|---|---|---|---|---|
| **PTZ1** | 4 | 291700 | T | C | intergenic_region | gene_7501-gene_7502 | NA | CHAT domain | intergenic |
| **PTZ2** | 4 | 289147 | T | C | intergenic_region | gene_7501-gene_7502 | NA | CHAT domain | intergenic |
| **PTZ3** | 2 | 8826325 | A | C | upstream_gene_variant | gene_7332 | NA | Heterokaryon incompatibility | upstream |
| **PTZ3** | 3 | 5127051 | A | C | intergenic_region | gene_11981-gene_11982 | NA | Complex 1 LYR protein | intergenic |
| **PTZ3** | 4 | 289147 | T | C | intergenic_region | gene_7501-gene_7502 | NA | NA | intergenic |
| **PTZ4** | 4 | 284768 | T | C | intergenic_region | gene_7501-gene_7502 | NA | CHAT domain | intergenic |
| **TBF1** | 1 | 1888761 | G | C | upstream_gene_variant | gene_696 | NA | Zinc finger, C2H2 | upstream |
| **TBF1** | 2 | 6549594 | T | C | downstream_gene_variant | gene_6530 | NA | Hydrophobin | downstream |
| **TBF3** | 3 | 4409846 | T | C | intergenic_region | gene_11744-gene_11745 | NA | NB-ARC | intergenic |
| **TBF4** | 3 | 4434649 | T | C | intergenic_region | gene_11744-gene_11745 | NA | NB-ARC | intergenic |
| **TBF4** | 3 | 4434666 | T | C | intergenic_region | gene_11744-gene_11745 | NA | NB-ARC | intergenic |
| **TBF4** | 4 | 5081556 | CAGATCCCACTCCTCG | C | conservative_inframe_deletion | gene_9240 | p.Arg138_Ser142del | GNAT domain | indel |
| **PTZ1** | 1 | 290198 | TT | CC | intergenic_region | gene_94-gene_95 | NA | NA | intergenic |
| **TBF4** | 2 | 6544770 | TA | CG | intergenic_region | gene_6529-gene_6530 | NA | Hydrophobin | intergenic |
| **CMB1** | 1 | 9330706 | A | G | missense_variant | gene_3240 | p.Ser242Gly | NA | nonsynonymous |
| **CMB3** | 2 | 5751869 | A | G | 5_prime_UTR_variant | gene_6204 | NA | Predicted dehydrogenase, Secondary metabolites biosynthesis, transport and catabolism , Short-chain dehydrogenase/reductase SDR, 3-oxoacyl-[acyl- | UTR |

| | | | | | | | | | |
|---|---|---|---|---|---|---|---|---|---|
| | | | | | | | | carrier protein] reductase., Fatty acid biosynthesis (path 1) | |
| **DMS1** | 1 | 8203909 | GCCAGGGCCGAGGAGGAGC | G | disruptive_inframe_deletion | gene_2867 | p.Gln828_Ala833del | Translation initiation factor 3, subunit c (eIF-3c), Translation, ribosomal structure and biogenesis , Proteasome component (PCI) domain | indel |
| **DMS3** | 1 | 290111 | A | G | intergenic_region | gene_94-gene_95 | NA | NA | intergenic |
| **DMS3** | 1 | 290119 | A | G | intergenic_region | gene_94-gene_95 | NA | NA | intergenic |
| **PTZ1** | 1 | 290193 | A | G | intergenic_region | gene_94-gene_95 | NA | NA | intergenic |
| **PTZ1** | 4 | 291703 | A | G | intergenic_region | gene_7501-gene_7502 | NA | CHAT domain | intergenic |
| **PTZ2** | 4 | 287489 | A | G | intergenic_region | gene_7501-gene_7502 | NA | CHAT domain | intergenic |
| **PTZ3** | 3 | 4427974 | A | G | intergenic_region | gene_11744-gene_11745 | NA | Complex 1 LYR protein | intergenic |
| **PTZ3** | 4 | 284748 | A | G | intergenic_region | gene_7501-gene_7502 | NA | CHAT domain | intergenic |
| **PTZ4** | 3 | 8002755 | A | G | upstream_gene_variant | gene_12990 | NA | Kinesin light chain, Cytoskeleton , NB-ARC | upstream |
| **PTZ4** | 4 | 287489 | A | G | intergenic_region | gene_7501-gene_7502 | NA | CHAT domain | intergenic |
| **TBF2** | 1 | 294541 | A | G | upstream_gene_variant | gene_95 | NA | NA | upstream |
| **TBF2** | 3 | 6004930 | T | G | synonymous_variant | gene_12266 | p.Arg543Arg | Membrane coat complex Retromer, subunit VPS5/SNX1, Sorting nexins, and related PX domain-containing proteins, | synonymous |

| | | | | | | | | | |
|---|---|---|---|---|---|---|---|---|---|
| | | | | | | | | Intracellular trafficking, secretion, and vesicular transport , Phox homologous domain | |
| **TBF3** | 1 | 8776659 | A | G | splice_region_variant&intron_variant | gene_3076 | NA | Cyclin, General function prediction only , Cyclin PHO80-like | intergenic |
| **TBF4** | 1 | 8658710 | C | G | upstream_gene_variant | gene_3030 | NA | NA | upstream |
| **PTZ4** | 3 | 8002763 | AT | GC | upstream_gene_variant | gene_12990 | NA | Kinesin light chain, Cytoskeleton , NB-ARC | upstream |
| **TBF4** | 1 | 3483233 | G | GTCGAGGGATCGT | disruptive_inframe_insertion | gene_1217 | p.Ser1546_Arg1547insArgAspArgSer | NA | indel |
| **CMB4** | 4 | 288700 | C | T | intergenic_region | gene_7501-gene_7502 | NA | CHAT domain | intergenic |
| **DMS1** | 4 | 3666625 | G | T | downstream_gene_variant | gene_8727 | NA | NA | downstream |
| **DMS1** | 4 | 6820154 | TTCTATCA | T | frameshift_variant | gene_9847 | p.Ser328fs | Zinc-binding oxidoreductase, Energy production and conversion , Alcohol dehydrogenase GroES-like, NADPH:quinone reductase., \N | nonsynonymous |
| **DMS2** | 4 | 5636482 | G | T | missense_variant | gene_9408 | p.Met290Ile | NA | nonsynonymous |
| **DMS3** | 1 | 11264658 | G | T | stop_gained | gene_3914 | p.Glu3823* | Non-ribosomal peptide synthetase/alpha-aminoadipate reductase and related enzymes, Secondary metabolites biosynthesis, transport and | nonsynonymous |

| | | | | | | | | | |
|---|---|---|---|---|---|---|---|---|---|
| | | | | | | | | catabolism , AMP-dependent synthetase/ligase | |
| **DMS3** | 2 | 1601101 | C | T | upstream_gene_variant | gene_4688 | NA | NA | upstream |
| **DMS3** | 3 | 4648180 | C | T | missense_variant | gene_11819 | p.Val457Met | NA | nonsynonymous |
| **DMS4** | 2 | 7517692 | C | T | missense_variant | gene_6875 | p.Pro369Ser | RNA polymerase II elongator complex, subunit ELP4, Chromatin structure and dynamics , Elongator complex protein 4 | nonsynonymous |
| **DMS4** | 4 | 69767 | A | T | downstream_gene_variant | gene_7427 | NA | NA | downstream |
| **DMS4** | 4 | 69773 | C | T | downstream_gene_variant | gene_7427 | NA | NA | downstream |
| **DMS4** | 4 | 7812624 | TATTG | T | upstream_gene_variant | gene_10241 | NA | GNAT domain | upstream |
| **PTZ1** | 1 | 9023851 | G | T | intergenic_region | gene_3145-gene_3146 | NA | RNA polymerase III, large subunit, Transcription , RNA polymerase, alpha subunit, DNA-directed RNA polymerase., RNA polymerase | intergenic |
| **PTZ1** | 4 | 3515952 | G | T | synonymous_variant | gene_8664 | p.Pro174Pro | Peptidase S8/S53 domain, Serine endopeptidases., \N | synonymous |
| **PTZ2** | 1 | 1189467 | C | T | synonymous_variant | gene_444 | p.Ser763Ser | Predicted hydrolase involved in interstrand cross-link repair, Replication, recombination and repair , DNA repair metallo-beta-lactamase | synonymous |
| **PTZ2** | 4 | 288700 | C | T | intergenic_region | gene_7501-gene_7502 | NA | CHAT domain | intergenic |
| **PTZ2** | 4 | 4159757 | G | T | missense_variant | gene_8915 | p.Lys493Asn | ATP-citrate lyase, Energy production | nonsynonymous |

| | | | | | | | | | |
|---|---|---|---|---|---|---|---|---|---|
| | | | | | | | | and conversion , Citrate synthase-like | |
| **TBF1** | 2 | 4807361 | A | T | synonymous_variant | gene_5820 | p.Gly500Gly | FAD linked oxidase, N-terminal | synonymous |
| **TBF1** | 4 | 5431413 | A | T | intergenic_region | gene_9348-gene_9350 | NA | NA | intergenic |
| **TBF2** | 1 | 8989741 | A | T | intergenic_region | gene_3145-gene_3146 | NA | RNA polymerase III, large subunit, Transcription , RNA polymerase, alpha subunit, DNA-directed RNA polymerase., RNA polymerase | intergenic |
| **TBF2** | 1 | 8989746 | G | T | intergenic_region | gene_3145-gene_3146 | NA | RNA polymerase III, large subunit, Transcription , RNA polymerase, alpha subunit, DNA-directed RNA polymerase., RNA polymerase | intergenic |
| **TBF2** | 3 | 5092367 | A | T | intergenic_region | gene_11981-gene_11982 | NA | Complex 1 LYR protein | intergenic |
| **TBF2** | 4 | 286522 | C | T | intergenic_region | gene_7501-gene_7502 | NA | CHAT domain | intergenic |
| **TBF2** | 4 | 286522 | C | T | missense_variant | gene_8994 | p.Gly199Ser | Mitochondrial carrier domain | nonsynonymous |
| **TBF3** | 1 | 2832715 | C | T | synonymous_variant | gene_996 | p.Lys71Lys | NA | synonymous |
| **TBF3** | 3 | 5103303 | A | T | intergenic_region | gene_11981-gene_11982 | NA | Complex 1 LYR protein | intergenic |
| **TBF4** | 1 | 3801230 | TCTCAAATC | T | upstream_gene_variant | gene_1326 | NA | 60S ribosomal protein L9, Translation, ribosomal structure and biogenesis , Ribosomal protein L6, alpha-beta domain | upstream |

| | | | | | | | | | |
|---|---|---|---|---|---|---|---|---|---|
| **TBF1** | 4 | 2746703 | T | TA | frameshift_variant | gene_8383 | p.Ser102fs | SMT3/SUMO-activating complex, AOS1/RAD31 component, Posttranslational modification, protein turnover, chaperones , UBA/THIF-type NAD/FAD binding fold, Ubiquitin--protein ligase., \N | nonsynonymous |
| **TBF4** | 4 | 5401729 | CT | TA | upstream_gene_variant | gene_9346 | NA | E3 ubiquitin protein ligase, Posttranslational modification, protein turnover, chaperones , HECT | upstream |
| **TBF2** | 1 | 294547 | CC | TT | upstream_gene_variant | gene_95 | NA | NA | upstream |
| **PTZ4** | 2 | 6318655 | T | TTG TTA AGC GAG ATT ACT TGG AAA AGG AAC | frameshift_variant | gene_6436 | p.Val429fs | Proteins containing the FAD binding domain, Energy production and conversion , FAD linked oxidase, N-terminal, D-lactate dehydrogenase (cytochrome)., Pyruvate metabolism | nonsynonymous |

In the TBF1 lineage, a high-confidence genetic variant in the gene *smt3* (Mycocosm protein ID: 538900, gene ID: gene_8383) was identified, with exact correspondence between variant presence and the phenotypic pattern of reduced sensitivity to TBF. All timepoints in the TBF1 lineage from transfer 20 and following had a single base insertion that caused a premature stop codon at amino acid S102, while all strains from earlier timepoints in the lineage had the wild-type genotype. To confirm the phenotypic effect of this mutation, we engineered a *Δsmt3* deletion in the ancestral strain. Successful deletion of the *smt3* gene and insertion of a single copy of the hygromycin resistance gene were confirmed through qPCR and sanger sequencing. Two different knockout strains (*Δsmt3_1*, *Δsmt3_2*) both phenocopied the evolved TBF1 lineage for tebuconazole resistance (Figure 2.6A) and macroconidia phenotype (Figure 2.6B), suggesting that the observed mutation is responsible for both observed phenotypes through gene loss-of-function. The *smt3* gene is predicted to be important for maintaining macroconidia dormancy until ideal germination conditions arise.

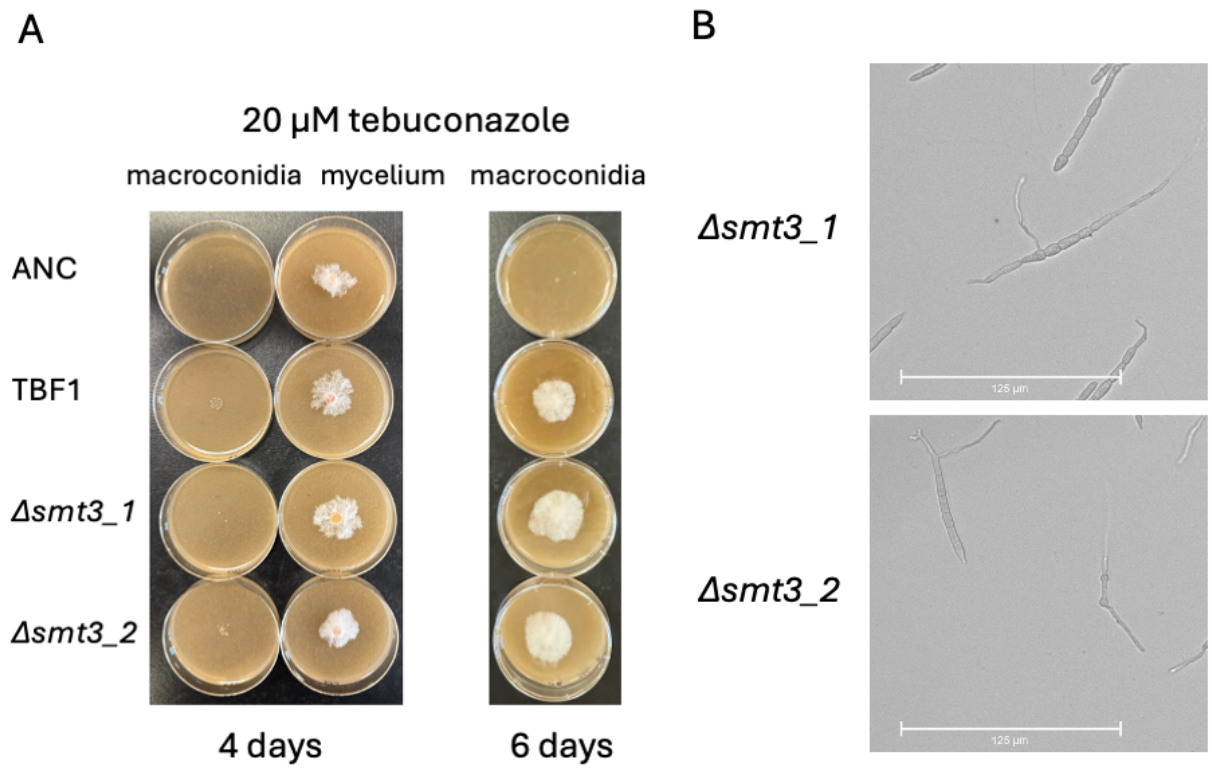


**Figure 2.6 Phenotyping assay of the *Δsmt3* strains. A. Assay for growth in the presence of tebuconazole, when cultures were initiated with macroconidia or with actively growing mycelium. Four strains were tested: the ancestral strain, the evolved strain TBF1, and two deletion mutant strains, *Δsmt3_1* & *Δsmt3_2*. Photographs were taken after 4 and 6 days. B. Images of macroconidia from *Δsmt3_1* and *Δsmt3_2* deletion strains after 48 hours at 4 °C suspended in sterile water at a concentration of 0.5 macroconidia/µL. See Figure 2.4 for macroconidia of the ancestral and TBF1.**

# Discussion

The increasing use of fungicides paired with the observation in some jurisdictions of increasing antimicrobial resistance in agricultural pathogens, including *F. graminearum* (Toda et al., 2021), highlights the critical need to better understand the dynamics of fungicide-driven evolution in populations of fungal pathogens. To study this directly, we evolved replicate lineages of *F. graminearum* to three different drug treatments: increasing prothioconazole, increasing tebuconazole, and an increasing combination of the two drugs. All evolved lineages demonstrated the ability to grow at azole concentrations well exceeding the initial MIC, demonstrating a response to the selective pressure imposed by azole exposure.

The degree of growth improvement differed by treatment. Based on the well-established principle that multi-drug regimens are often more effective at preventing resistance development in bacterial infections (Vivas et al., 2019), we expected less effective evolution around the combination treatment, compared to the individual drugs. This principle is also applied in agricultural fungicide formulations, with products such as Prosaro PRO (Bayer Crop Science) including a combination of prothioconazole and tebuconazole (*Prosaro® PRO Fungicide*, n.d.). Indeed, consistent with this expectation, lineages exposed solely to prothioconazole or to tebuconazole exceeded the initial MIC by 4× and 5.1× respectively, while the combined treatment lineages only exceeded the initial MIC by 2.5×. This suggests that the simultaneous exposure to two different azoles, which interact with different portions of the same target protein, imposes a more stringent selective pressure. This finding reinforces the value of combination fungicides in resistance management strategies.

However, with the notable exception of the TBF1 lineage, the phenotype of enhanced resistance was largely lost after storage at -80 ℃ and subsequent re-testing from macroconidia. This instability, coupled with the absence of significant, stable genetic alterations in known targeted genes in these lineages suggests the involvement of non-genetic factors. The phenomenon by which exposure to a stress leads to an enhanced response upon subsequent exposure to related stressors is referred to as 'priming' in the fungal literature (Harish et al., 2022; Hilker et al., 2016). A recent study investigated the priming effect in *F. graminearum* in response to tebuconazole and metconazole found that conidia exposed to a partially inhibitory concentration of fungicide exhibited significantly higher germination rates and longer hyphal lengths when subsequently exposed to a doubled fungicide concentration, compared to unprimed

conidia (Wang et al., 2025). The priming effect was linked to overexpression of the *cyp51* genes, with regulatory influence by the transcription factor FgSR, which is itself regulated through SUMOylation (Wang et al., 2025). The priming effect was retained for up to 30 days, but was not stably heritable once the fungicide stress was removed (Wang et al., 2025). Epigenetic mechanisms are increasingly recognized as key regulators of fungal biology, influencing development, phenotypic plasticity and the acquisition of antifungal resistance (Buscaino, 2019; Chang et al., 2019; Kuchler et al., 2016; Y. Li et al., 2019; Madhani, 2021; O'Kane et al., 2020). The observed transient nature of growth improvement under persistent azole exposure in most of our evolved *F. graminearum* lineages is very similar to observations from a recently published laboratory directed evolution experiment involving *Candida albicans* and the broad spectrum antimicrobial boric acid (Syvolos et al., 2024). Given the biological and biochemical differences between these two species and drugs, this suggests that unstable, non-mutational changes may be a more common phenomenon enabling fungi to grow under high drug exposure when the drug selective pressure is applied in an increasing fashion. Further work is needed to deeply characterize the interplay between adaptation and epigenetic acclimation under different drug dosing regimens in diverse species.

Interestingly, our data indicate a pronounced difference in the sensitivity toward azoles of *F. graminearum* macroconidia vs. mycelium; a lower concentration of tebuconazole or prothioconazole was required to inhibit macroconidia germination compared to inhibition of mycelial elongation. In another study with the fungicide pydiflumetofen, the opposite was seen, where the $EC_{50}$ value to inhibit *F. graminearum* spore germination was just over double the amount needed to inhibit mycelial elongation (Breunig & Chilvers, 2021). More work is needed to understand interactions between fungicide exposure and spore germination, as such effects have significant practical field implications. For example, fungicides that are stronger inhibitors of germination should be used preventatively before fungal pathogens have established, while fungicides that are stronger inhibitors of mycelial elongation may be more effective after pathogen establishment.

In contrast to the other evolved strains, TBF1 presented a stable, heritable phenotype of decreased azole sensitivity, particularly when macroconidia were exposed to the azoles. The evolved TBF1 strain was also the only phenotypic outlier for the other traits we examined, exhibiting altered macroconidia dormancy. Both phenotypes were linked to a nonsense mutation

in *smt3*. The s*mt3* gene codes for a small ubiquitin-like modifier (SUMO) protein which is used for posttranslational modifications (Gupta et al., 2020). In *Candida albicans*, SUMOylation plays a role in the DNA damage repair response (Islam et al., 2019), and *SMT3* is important in cell growth, cell division, and tolerance to external stressors such as oxidation and response to azoles (Leach et al., 2011). The deletion of the *smt3* gene in *Aspergillus nidulans* yields impaired growth and conidiation and causes sterility (Wong et al., 2008).

Previous work done on *smt3* in *F. graminearum* found that a *Δsmt3* knock-out strain performed as well as the reference strain in the presence of tebuconazole, and transcription of *cyp51A* and *cyp51B* was not impacted, even though the *smt3* gene is involved in the SUMOylation of the *cyp51* genes in the ergosterol biosynthesis pathway (Jian et al., 2023). However, it is notable that Jian et al. used actively growing mycelium in their azole sensitivity assay; it is only when macroconidia are exposed to drug that the resistance-conferring effect of the loss of *smt3* function becomes evident. A gene expression analysis of the *smt3* gene in the related species *Fusarium oxysporum* indicated that the expression of SUMOylation-related genes *smt3*, *aos1*, and *mms21* is significantly elevated in germinating macroconidia compared to in mycelium (Azizullah et al., 2023). At the same time, their *Δsmt3* mutants in *F. oxysporum* suffered low germination rates (Azizullah et al., 2023), which is opposite to the spontaneous and accelerated germination observed in *F. graminearum* in our study. Deciphering the mechanisms for the different impact of disruption of *smt3* function across these two species would improve our understanding of fungal cell biology and of spore dormancy and spore germination processes.

The *smt3* gene is highly expressed in germinated macroconidia of *Fusarium oxysporum* and not in mycelial growth, suggesting that loss of *smt3* may cause macroconidia to behave like mycelium. This may include a lack of perception of or response to environmental cues that would typically hold macroconidia in a dormant state. F. *graminearum* macroconidia germinate under particular environmental conditions (i.e., humidity, warm temperatures, and nutrients available; see Figure S4 A). When these conditions are not met (i.e., dry, cold, lack of nutrients), F. *graminearum* macroconidia remain dormant (Figure S4 B). In the case of the *Δsmt3* or the evolved TBF1 strain, however, macroconidia germinate regardless of the surrounding environmental state, including both stressful conditions (azole exposure) and conditions that would typically stimulate production of macroconidia (e.g., growth in CMC broth; Figure S4 C).

Additional research to understand the role that the *smt3* gene plays in macroconidia germination cues would be fruitful. A study on *F. graminearum* evaluated gene expression at 0, 2, 8 and 24 hours post germination found over 5,000 genes being expressed at each time point, showing the complexity of the germination process and the number of genes that are involved in germination (Seong et al., 2008).

Features of the design of our evolution experiment may have contributed to the preponderance of unstable phenotypic responses to stressful exposure to azoles that we observed. Our evolution experiment was conducted on solid media, differing from other laboratory evolution experiments that have been conducted in liquid media, which provides more uniform exposure to the azole (Rayko et al., 2010). We chose a solid medium to more closely simulate the growth of the fungus on a plant having only surface azole contact, for the ability to quantify growth rates easily throughout the duration of the experiment, and to be able to intentionally advance cells with apparent beneficial mutations (i.e., deliberately selecting colony sectors with faster growth). However, this approach may have inadvertently reduced the intensity of selection pressures on the fungal population. For example, mycelial growth on solid surfaces can allow portions of the fungal colony to grow upwards or away from direct contact with the azole in the agar. This escape mechanism could dilute the selection intensity, therefore limiting the rate at which a strong target site mutations are fixed in the population. To avoid selecting for mutations that would have severe fitness costs in a natural setting, and to make it more likely that heritable phenotypic responses were being observed, our evolving lineages were passed through a macroconidia production stage after every five transfers. This process may, for example, have purged any mutations that would have abolished macroconidia production capacity. However, our choice to remove the azole exposure during spore production certainly impacted the selective environment as a whole, and may have led to the loss of some resistance-conferring mutations within the experimental populations.

It is important to consider the fitness of evolved strains that have mutations that confer antimicrobial resistance. In the case of the evolved TBF1 strain, mutation in the *smt3* gene provided reduced sensitivity through early spore germination, effectively switching the exposure to a scenario of actively growing mycelium, in which the MIC is higher. However, some degree of macroconidia dormancy is likely to be critical to survival through unfavorable environments or episodes, such as winter freezing or periods of drought. Furthermore, physical displacement of

spores, such as by wind or rain splash, is critical to effective dissemination of the pathogen to suitable infection courts (e.g., dispersing from crop debris at the soil surface to the flowering structures within the phylosphere). Therefore, the specific mutation observed in our evolution experiment, loss of function of *smt3*, is unlikely to be maintained in wild populations. However, our results suggest that a route toward fungicide resistance is available through alteration or fine-tuning of spore germination processes, an evolutionary trajectory that has rarely been considered in the context of antimicrobial resistance acquisition among fungal plant pathogens.

Fungicidal compounds kill the fungus, while fungistatic compounds only inhibit its growth and reproduction. The effect of a compound is often determined by its concentration. For example, a fungicide that is fungicidal at high concentrations may be fungistatic at lower concentrations. While a fungicidal action is ideal for complete disease control, many widely used fungicides, particularly azoles that target the ergosterol biosynthesis pathway through the gene *cyp51* or *Erg11* (yeast species), are primarily fungistatic (Kumar et al., 2018). This fungistatic mode of action provides a critical opportunity for pathogens to evolve and adapt. Instead of being eliminated, the fungal population is merely suppressed, allowing a subpopulation of cells to survive the selective pressure. These surviving cells may possess pre-existing mutations or develop new, often transient, physiological or epigenetic mechanisms that enable them to tolerate the fungicide. For example, some fungi can temporarily increase the expression of efflux pumps to expel the drug from their cells or alter the fungicide's target site to reduce its binding affinity (Hahn, 2014). This temporary survival under fungistatic pressure can pave the way for the accumulation of more stable, heritable genetic changes that confer permanent resistance. This phenomenon is supported by research showing that fungistatic drugs can actually promote the development of resistance more effectively than fungicidal ones because they leave a viable, albeit stressed, population to evolve (Cowen, 2008). Therefore, the widespread use of fungistatic compounds creates a fertile ground for the evolution of resistance, highlighting the need for strategic application and the development of new fungicidal drugs. Work from this study highlights the variation in fungicide capabilities to inhibit macroconidia germination, compared to mycelial elongation, the importance of the presence of epigenetics that could affect in season fungicide resistance, and a putative mutation site that confers azole resistance.

## Acknowledgements

Acknowledgements to Dr. Sean Walkowiak for the support and guidance in the variant calling work, and to Dr. Anuradha Jayathissa for the guidance in the creation of the CRISPR Cas9 gene deletions. This work was supported by NSERC Discovery Grants RGPIN-2020-05334 and ACG NSERC Discovery Grant, and by the Governments of Canada and of Manitoba, the Manitoba Crop Alliance, and the Western Grains Research Foundation as Sustainable Canadian Agricultural Partnership task #T01022. Results and conclusions presented here are not official positions of the Governments of Canada or of Manitoba. The EvoFunPath training program provided support and training for K. Wog.

# Chapter 3 - Discussion

*Fusarium graminearum* is a devastating agricultural pathogen, managed by farmers with integrated management strategies to reduce the incidence of disease. While azoles have been highly effective in managing this major pathogen, the repeated exposure of fungal populations to these compounds has created a strong selective pressure for the development of resistance.

Experimental evolution has emerged as a powerful tool for studying the genetic basis of phenotypes of interest such as drug resistance. By subjecting replicate microbial populations to a controlled selective pressure in a laboratory setting, researchers can observe and analyze the evolutionary process in real time. This approach has been widely and successfully applied to study of human pathogenic fungi, providing important insights into the genetic pathways and adaptive strategies that enable resistance to clinical antifungals (Gerstein & Sethi, 2022).

The primary goal of this thesis was to use experimental evolution with an agriculturally significant pathogen, *F. graminearum*, to identify the genetic and phenotypic changes that confer resistance to azole fungicides. Our results, which demonstrate a novel non-*cyp51* resistance mechanism, provide new insight to fungicide resistance and highlight the importance of considering alternative genetic pathways that may contribute to enhanced resistance.

Although we did not directly study epigenetics, but in theory and based on the literature, epigenetics likely played a role in the phenotype of unstable resistance (Harish et al., 2022). Therefore, conducting further research on the potential role of epigenetic changes through gene expression assays, and studying DNA methylation would be a valuable next step. With practical applications, a future study looking into epigenetic factors such as DNA methylation, histone modification, and gene expression throughout a growing season on fields could provide insight into effective fungicide protocols that will not induce priming of the fungal colonies in the field. With the results in this study mostly showing non-genetic adaptation to increasing concentrations of azoles, performing gene expression assays at each timepoint could provide insight into up- or down-regulation of genes to determine which ones are linked to azole tolerance. Results from a gene expression assay of an evolved strain compared to the ancestral strain could potentially show an upregulation of stress response genes, drug efflux pump genes, and *cyp51A & B* genes compared to the ancestral.

One of the most surprising results from this experiment was the phenotypic instability of azole resistance. This suggests that epigenetics may play a role in enabling species to acclimate to azole exposure without genetic changes (i.e., rather than adapt). Related to this is the concept of priming. Priming refers to the phenomenon in which exposure to a stress leads to an enhanced adaptive response upon subsequent exposure to related stressors (Harish et al., 2022; Hilker et al., 2016). This ability to "remember" past encounters, while often transient, allows for more effective response to future challenges. A recent study investigated the priming effect in *F. graminearum* in response to the azole fungicides tebuconazole and metconazole (Wang et al., 2025). They found that compared to unprimed conidia, conidia exposed to an effective concentration of fungicide ($EC_{50}$; i.e., the drug concentration that inhibits 50% of growth) exhibited significantly higher germination rates and longer hyphal lengths when subsequently exposed to double the $EC_{50}$ (Wang et al., 2025). They determined that the priming effect was retained in conidia for up to 30 days, but was not stably heritable indefinitely once the fungicide stress was removed (Wang et al., 2025). This non-heritable nature suggests that the priming effect is mediated by epigenetic mechanisms rather than stable mutations (Guan et al., 2012; Horsthemke, 2018). In the field, fungicide exposure during one part of the season could trigger epigenetic changes that help the fungus survive later applications. With the transient nature of priming and epigenetics, the resistant phenotypes likely do not persist through the winter or from one season to the next. This means that a new season of fungicide exposure might lead to the development of new, season-specific tolerance, rather than the accumulation of stable resistance. This presents a unique challenge, since with genetic resistance, there is potential for different (susceptible) genes/pathways to be targeted.

In contrast to most prior fungal studies of experimental evolution in yeast species, we evolved *F. graminearum* on agar plates due to the filamentous nature of the fungus. An interesting phenotype arose rapidly during the evolution experiment in all of the prothioconazole-evolved lineages— vertical mycelial growth, presumably as a mechanism for cells to minimize contact with the antifungal drug (Figure S3). This phenotype was only observed in the presence of prothioconazole alone, not in the combination treatment with tebuconazole and prothioconazole. This response to prothioconazole exposure must have resulted from an environmental sensing mechanism, the details and genetic basis of which it would be very interesting to untangle. As soon as the prothioconazole-evoled strains were placed

on azole-free media, they exhibited normal growth, i.e., lateral flat growth on the surface of the plate. This suggests that the response is also directly triggered by the presence of prothioconazole or its active metabolite, prothioconazole-desthio, rather than resulting from a permanent genetic change. This is an interesting example of how a stressor can induce a rapid and highly specific physiological change in a filamentous fungus. The ability to sense and physically escape a chemical stressor is a novel form of tolerance that could be relevant in agricultural settings, particularly in a solid substrate like a wheat head. For example, if fungicide application is not entirely homogenous, the fungus may be able to preferentially colonize tissues or microsites with lower fungicide loads. The underlying mechanism for this sensory response and the subsequent change in growth direction remains an open question for future research.

The *smt3* single-base insertion in the TBF1 lineage arose in transfer 20, when the azole concentration was 6.4 μM, which is below the ancestral MIC. This insertion was maintained through the remainder of the evolution experiment, indicating it likely did not cause a reduction in fitness. In the context of the evolution experiment, TBF1 did not appear to distinguish itself from the other tebuconazole evolved lineages, performing equally in terms of growth area. During the evolution experiment, the putative epigenetic changes in the other tebuconazole-evolved lineages and the *smt3* mutation in TBF1 presented phenotypically identical, leading to the question of how much epigenetics factored into lineage TBF1, or if the *smt3* mutation minimized the need for epigenetic changes.

This experiment's findings on the different effects of the same concentration of azoles on macroconidia versus mycelial growth offer important insight for applications in the field. A much lower concentration of azole is needed to inhibit macroconidia germination than mycelial elongation. This differs from pydiflumetofen, where a lower concentration is needed to inhibit mycelial elongation (Breunig & Chilvers, 2021). Understanding the fungicide, and the disease infection stage a field is in, could help farmers more effectively manage fungal outbreaks. For example, a lower concentration of azole could be used as a preventive measure if it is known that there are potentially macroconidia in the field. Once an infection has been established, it would be a better choice to use a higher concentration of azole (or a different drug class) to inhibit or control mycelium growth.

Multi-drug use is proven to have synergistic effects, shown by the use of tebuconazole and prothioconazole in combination in Proline Pro by Bayer CropScience, as well as medical

applications in the clinic. In this experiment, tebuconazole and prothioconazole were used in combination equally at a molecular level, yet the MIC's for each azole solely were much different. Another modification to this study that could be of interest is adjusting the ratio of each azole, to find a balance where in combination, the least amount of total drug is needed.

Our experiments used the lab-cultured *F. graminearum* reference strain (DAOMC 233423), which represents a genetically uniform population. We found that our ancestral strain had thousands of genetic variants compared to the published reference genome (z3639 v4) from Mycocosm, likely due to the accumulation of mutations during its extensive time in laboratory cultivation. While this controlled approach allows for precise experimental manipulation, it only partially models the multifaceted selective pressures that would be found in a field setting, as well as the high genetic diversity of field populations of *F. graminearum* (Walker et al., 2025). Therefore, a more direct and representative model of pathogen evolution could be achieved by using a recently isolated, genetically diverse small population, providing more genetic diversity from the beginning of the evolution experiment.

There are many ways to do experimental evolution. The methodology selected in this study of plate transfers was selected to be able to quantify growth rate after each transfer through images, and to be continuously selecting mycelium that grew vigorously (taking a plug from the leading edge of the growth front). By conducting transfers with vigorous mycelium, there was a greater chance to eliminate populations that acquired mutations with fitness costs. Initially, before conducting the evolution experiment on Petri plates, the goal was to conduct the experiment in glass race tubes, allowing for continuous linear mycelial growth, hoping to have the most fit populations reach the end of the tube first. However, that approach suffered from contamination issues and a gradual desiccation of the growth media. A modification to this methodology could be conducting the experiment in liquid culture. This methodology would ensure that all cells are continuously exposed to the antifungal selection pressure, preventing the physical escape of mycelium from the media, as was observed with the vertical growth phenotype in the prothioconazole-treated lineages. Additionally, this approach would more effectively expose the macroconidia-producing stage to the fungicide stress, potentially leading to different mutational outcomes.

Another modification would be moving *F. graminearum* through an evolution experiment that involves frequent passage through meiosis. During the evolution experiment that

was conducted, *F. graminearum* only replicated cells through mitosis, which eliminates genetic recombination which happens during meiosis. Although difficult to achieve in a lab setting, an experiment that includes forced continual sexual reproduction through perithecia, would be highly valuable. An experiment like this would explore the potential role of recombination through meiosis in generating novel resistance phenotypes in the presence of selection pressures, as sexual reproduction happens in the field.

# Conclusion

This study applied a laboratory evolution methodology to investigate the mechanisms of azole resistance in the agricultural fungal pathogen, *Fusarium graminearum*. Our findings reveal that while all evolved lineages gained a transient increase in azole tolerance, only the TBF1 lineage developed a stable, heritable resistance. This stable resistance was not due to mutations in the canonical azole target gene *cyp51*, but instead was linked to a single base pair insertion in the *smt3* gene. This mutation caused a loss of gene function, leading to an altered macroconidia dormancy and quick germination process. The data suggests that epigenetic changes and phenotypic plasticity play a significant, but often temporary, role in fungal acclimation to stress, which is important for in season fungicide management. The stable resistance mutation in *smt3* represents a previously uncharacterized pathway to resistance, highlighting that fungal pathogens may use alternative, non-canonical mechanisms to evade chemical controls.

# References:

Abou Ammar, G., Tryono, R., Döll, K., Karlovsky, P., Deising, H. B., & Wirsel, S. G. R. (2013). Identification of ABC transporter genes of *Fusarium graminearum* with roles in azole tolerance and/or virulence. *PloS One*, *8*(11), e79042.

Azizullah, Noman, M., Gao, Y., Wang, H., Xiong, X., Wang, J., Li, D., & Song, F. (2023). The SUMOylation Pathway Components Are Required for Vegetative Growth, Asexual Development, Cytotoxic Responses, and Programmed Cell Death Events in *Fusarium oxysporum f. sp. niveum*. *Journal of Fungi (Basel, Switzerland)*, *9*(1), 94.

*Babraham Bioinformatics - FastQC A Quality Control tool for High Throughput Sequence Data*. (n.d.). Retrieved April 27, 2025, from https://www.bioinformatics.babraham.ac.uk/projects/fastqc/

Barrick, J. (2025). *80,000 Generations: New Olympic Record*. https://the-ltee.org/80000-generations-new-olympic-record/

Becher, R., Hettwer, U., Karlovsky, P., Deising, H. B., & Wirsel, S. G. R. (2010). Adaptation of *Fusarium graminearum* to tebuconazole yielded descendants diverging for levels of fitness, fungicide resistance, virulence, and mycotoxin production. *Phytopathology*, *100*(5), 444–453.

Bédard, C., Pageau, A., Fijarczyk, A., Mendoza-Salido, D., Alcañiz, A. J., Després, P. C., Durand, R., Plante, S., Alexander, E. M. M., Rouleau, F. D., Jordan, D. F., Jay, A., Giguère, M., Bernier, M., Sharma, J., Maroc, L., Gervais, N. C., Menon, A. C. T., Gagnon-Arsenault, I., … Landry, C. R. (2025). FungAMR: a comprehensive database for investigating fungal mutations associated with antimicrobial resistance. *Nature Microbiology*. https://doi.org/10.1038/s41564-025-02084-7

Benjamin, D., Sato, T., Cibulskis, K., Getz, G., Stewart, C., & Lichtenstein, L. (2019). Calling Somatic SNVs and Indels with Mutect2. In *bioRxiv* (p. 861054). https://doi.org/10.1101/861054

Berger, S., El Chazli, Y., Babu, A. F., & Coste, A. T. (2017). Azole Resistance in *Aspergillus fumigatus*: A Consequence of Antifungal Use in Agriculture? *Frontiers in Microbiology*, *8*, 1024.

Beyer, M., Röding, S., Ludewig, A., & Verreet, J.-A. (2004). Germination and Survival of *Fusarium graminearum* Macroconidia as Affected by Environmental Factors. *Journal of Phytopathology (1986)*, *152*(2), 92–97.

Bowden, R. L., & Leslie, J. F. (1999). Sexual recombination in *Gibberella zeae*. *Phytopathology*, *89*(2), 182–188.

Breunig, M., & Chilvers, M. I. (2021). Baseline sensitivity of *Fusarium graminearum* from wheat, corn, dry bean and soybean to pydiflumetofen in Michigan, USA. *Crop Protection (Guildford, Surrey)*, *140*(105419), 105419.

Broad Institute. (2019). *SortSam (Picard)*. GATK. https://gatk.broadinstitute.org/hc/en-us/articles/360037594291-SortSam-Picard

Broad Institute. (2020). *SamFormatConverter (Picard)*. GATK. https://gatk.broadinstitute.org/hc/en-us/articles/360037058992-SamFormatConverter-Picard

Broad Institute. (2024). *MarkDuplicates*. GATK. https://gatk.broadinstitute.org/hc/en-us/articles/360037052812-MarkDuplicates-Picard

Buscaino, A. (2019). Chromatin-mediated regulation of genome plasticity in human fungal pathogens. *Genes*, *10*(11), 855.

Castiblanco, V., Castillo, H. E., & Miedaner, T. (2020). Be flexible and adapt easily—The great role of plasticity relative to genetic variation for aggressiveness of *Fusarium culmorum* isolates. *Journal of Phytopathology*, *168*(3), 162–174.

Chang, Z., Yadav, V., Lee, S. C., & Heitman, J. (2019). Epigenetic mechanisms of drug resistance in fungi. *Fungal Genetics and Biology: FG & B*, *132*(103253), 103253.

Chen, A.-H., Islam, T., & Ma, Z.-H. (2022). An integrated pest management program for managing fusarium head blight disease in cereals. *Journal of Integrative Agriculture*, *21*(12), 3434–3444.

Chen, J., Wei, J., Fu, L., Wang, S., Liu, J., Guo, Q., Jiang, J., Tian, Y., Che, Z., Chen, G., & Liu, S. (2021). Tebuconazole resistance of *Fusarium graminearum* field populations from wheat in Henan Province. *Journal of Phytopathology (1986)*, *169*(9), 525–532.

Chunquan, S., Zhenyuan, M., Haitao, J., Jianzhong, Y., Wenya, W., Xiaoying, C., Guoqiang, D., Jiaguo, L., Wei, G., & Wannian, Z. (2009). Three-Dimensional Model of Lanosterol 14α-Demethylase from *Cryptococcus neoformans*: Active-Site Characterization and Insights into Azole Binding. *American Society for Microbiology*, *53*(8). https://doi.org/10.1128/aac.01630-08

Cooper, V. S. (2018). Experimental evolution as a high-throughput screen for genetic adaptations. *mSphere*, *3*(3). https://doi.org/10.1128/mSphere.00121-18

Cowen, L. E. (2008). The evolution of fungal drug resistance: modulating the trajectory from genotype to phenotype. *Nature Reviews. Microbiology*, *6*(3), 187–198.

*CreateSequenceDictionary (Picard)*. (2019). GATK. https://gatk.broadinstitute.org/hc/en-us/articles/360036347452-CreateSequenceDictionary-Picard

Cuomo, C. A., Güldener, U., Xu, J.-R., Trail, F., Turgeon, B. G., Di Pietro, A., Walton, J. D., Ma, L.-J., Baker, S. E., Rep, M., Adam, G., Antoniw, J., Baldwin, T., Calvo, S., Chang, Y.-L., Decaprio, D., Gale, L. R., Gnerre, S., Goswami, R. S., … Kistler, H. C. (2007). The Fusarium graminearum genome reveals a link between localized polymorphism and pathogen specialization. *Science (New York, N.Y.)*, *317*(5843), 1400–1402.

Duan, Y., Li, M., Zhao, H., Lu, F., Wang, J., & Zhou, M. (2018). Molecular and biological characteristics of laboratory metconazole-resistant mutants in *Fusarium graminearum*. *Pesticide Biochemistry and Physiology*, *152*, 55–61.

Edwards, S. G., & Godley, N. P. (2010). Reduction of Fusarium head blight and deoxynivalenol in wheat with early fungicide applications of prothioconazole. *Food Additives & Contaminants. Part A, Chemistry, Analysis, Control, Exposure & Risk Assessment*, *27*(5), 629–635.

E. Mellado, T. M. Diaz-Guerra, M. Cuenca-Estrella, J. L. Rodriguez-Tudela. (2001). Identification of Two Different 14-α Sterol Demethylase-Related Genes (cyp51A and cyp51B) in *Aspergillus fumigatus* and Other *Aspergillus* species. *American Society for Microbiology*, *39*(7). https://doi.org/10.1128/jcm.39.7.2431-2438.2001

Fan, J., Urban, M., Parker, J. E., Brewer, H. C., Kelly, S. L., Hammond-Kosack, K. E., Fraaije, B. A., Liu, X., & Cools, H. J. (2013). Characterization of the sterol 14α-demethylases of *Fusarium graminearum* identifies a novel genus-specific CYP51 function. *The New Phytologist*, *198*(3), 821–835.

FRAC. (2025a). *FRAC Mode of Action Group*. FRAC.

FRAC. (2025b). *Fungicide Resistance Management*. FRAC. https://www.frac.info/fungicide-resistance-management/#open-tour

Leonard. *Fusarium head blight of wheat and barley*. (2003). American Phytopathological Society.

Gagkaeva, T., Orina, A., & Gavrilova, O. (2021). Fusarium head blight in the Russian Far East: 140 years after description of the “drunken bread” problem. *PeerJ*, *9*(e12346), e12346.
Geng, Z., Zhu, W., Su, H., Zhao, Y., Zhang, K.-Q., & Yang, J. (2014). Recent advances in genes involved in secondary metabolite synthesis, hyphal development, energy metabolism and

pathogenicity in *Fusarium graminearum* (teleomorph *Gibberella zeae*). *Biotechnology Advances*, *32*(2), 390–402.

Gerstein, A. C., & Sethi, P. (2022). Experimental evolution of drug resistance in human fungal pathogens. *Current Opinion in Genetics & Development*, *76*(101965), 101965.

Guan, Q., Haroon, S., Bravo, D. G., Will, J. L., & Gasch, A. P. (2012). Cellular memory of acquired stress resistance in *Saccharomyces cerevisiae*. *Genetics*, *192*(2), 495–505.

Gupta, D., Garapati, H. S., Kakumanu, A. V. S., Shukla, R., & Mishra, K. (2020). SUMOylation in fungi: A potential target for intervention. *Computational and Structural Biotechnology Journal*, *18*, 3484–3493.

Hahn, M. (2014). The rising threat of fungicide resistance in plant pathogenic fungi: *Botrytis* as a case study. *Journal of Chemical Biology*, *7*(4), 133–141.

Harish, E., Sarkar, A., Handelman, M., Abo Kandil, A., Shadkchan, Y., Wurster, S., Kontoyiannis, D. P., & Osherov, N. (2022). Triazole priming as an adaptive response and gateway to resistance in *Aspergillus fumigatus*. *Antimicrobial Agents and Chemotherapy*, *66*(8), e0045822.

Hilker, M., Schwachtje, J., Baier, M., Balazadeh, S., Bäurle, I., Geiselhardt, S., Hincha, D. K., Kunze, R., Mueller-Roeber, B., Rillig, M. C., Rolff, J., Romeis, T., Schmülling, T., Steppuhn, A., van Dongen, J., Whitcomb, S. J., Wurst, S., Zuther, E., & Kopka, J. (2016). Priming and memory of stress responses in organisms lacking a nervous system. *Biological Reviews of the Cambridge Philosophical Society*, *91*(4), 1118–1133.

Hollomon, D. W. (2015). Fungicide resistance: 40 years on and still a major problem. In *Fungicide Resistance in Plant Pathogens* (pp. 3–11). Springer Japan.

Hollomon, K., & Brent, D. (1998). *FUNGICIDE RESISTANCE: THE ASSESSMENT OF RISK*. Global Crop Protection Federation.

*Home - Fusarium graminearum Z3639 v4.0*. (n.d.). Retrieved July 4, 2025, from https://mycocosm.jgi.doe.gov/Fusgra4/Fusgra4.home.html

Horsthemke, B. (2018). A critical view on transgenerational epigenetic inheritance in humans. *Nature Communications*, *9*(1), 2973.

H. W. Schroeder, J. J. C. (1964). Factors affecting resistance of wheat to scab caused by *Gibberella zeae*. *Phytopathology*, *53*(831), 38.

Islam, A., Tebbji, F., Mallick, J., Regan, H., Dumeaux, V., Omran, R. P., & Whiteway, M. (2019). Mms21: A putative SUMO E3 ligase in *Candida albicans* that negatively regulates invasiveness and filamentation, and is required for the genotoxic and cellular stress response. *Genetics*, *211*(2), 579–595.

Jian, Y., Chen, X., Sun, K., Liu, Z., Cheng, D., Cao, J., Liu, J., Cheng, X., Wu, L., Zhang, F., Luo, Y., Hahn, M., Ma, Z., & Yin, Y. (2023). SUMOylation regulates pre-mRNA splicing to overcome DNA damage in fungi. *The New Phytologist*, *237*(6), 2298–2315.

Jørgensen, L. N., & Heick, T. M. (2021). Azole use in agriculture, horticulture, and wood preservation - is it indispensable? *Frontiers in Cellular and Infection Microbiology*, *11*, 730297.

Klittich, C. J. (2008). Milestones in Fungicide Discovery: Chemistry that Changed Agriculture. *Plant Health Progress*, *9*(1), 31.

Kobayashi, K. (2019). Sexual reproduction and diversity: Connection between sexual selection and biological communities via population dynamics. *Population Ecology*, *61*(2), 135–140.
Kuchler, K., Jenull, S., Shivarathri, R., & Chauhan, N. (2016). Fungal KATs/KDACs: A new highway to better antifungal drugs? *PLoS Pathogens*, *12*(11), e1005938.

Kumar, A., Zarychanski, R., Pisipati, A., Kumar, A., Kethireddy, S., & Bow, E. J. (2018). Fungicidal versus fungistatic therapy of invasive *Candida* infection in non-neutropenic adults: a meta-analysis. *Mycology*, *9*(2), 116–128.

Labun, K., Montague, T. G., Krause, M., Torres Cleuren, Y. N., Tjeldnes, H., & Valen, E. (2019). *CHOPCHOP v3*. CHOPCHOP. https://chopchop.cbu.uib.no

LaCroix, R. A., Palsson, B. O., & Feist, A. M. (2017). A model for designing adaptive laboratory evolution experiments. *Applied and Environmental Microbiology*, *83*(8). https://doi.org/10.1128/aem.03115-16

Leach, M. D., Stead, D. A., Argo, E., & Brown, A. J. P. (2011). Identification of sumoylation targets, combined with inactivation of SMT3, reveals the impact of sumoylation upon growth, morphology, and stress resistance in the pathogen *Candida albicans*. *Molecular Biology of the Cell*, *22*(5), 687–702.

Lenski, R. E. (2003). Phenotypic and genomic evolution during a 20,000-generation experiment with the bacterium *Escherichia coli*. *Plant Breeding Reviews*, 225–265.

Lenski, R. E. (2017). Experimental evolution and the dynamics of adaptation and genome evolution in microbial populations. *The ISME Journal*, *11*(10), 2181–2194.

Leplat, J., Friberg, H., Abid, M., & Steinberg, C. (2013). Survival of *Fusarium graminearum*, the causal agent of Fusarium head blight. A review. *Agronomy for Sustainable Development*, *33*(1), 97–111.

Li H And Durbin. (2009). Fast and accurate short read alignment with Burrows-Wheeler Transform. *Bioinformatics*, *25*, 1754–1760.

Li, H., Whitwham, A., & Davies, R. (2025). *Samtools Manual*. Samtools. https://www.htslib.org/doc/samtools-faidx.html

Li, Y., Li, H., Sui, M., Li, M., Wang, J., Meng, Y., Sun, T., Liang, Q., Suo, C., Gao, X., Li, C., Li, Z., Du, W., Zhang, B., Sai, S., Zhang, Z., Ye, J., Wang, H., Yue, S., … Ding, C. (2019). Fungal acetylome comparative analysis identifies an essential role of acetylation in human fungal pathogen virulence. *Communications Biology*, *2*(1), 154.

Lockhart, S. R., Chowdhary, A., & Gold, J. A. W. (2023). The rapid emergence of antifungal-resistant human-pathogenic fungi. *Nature Reviews. Microbiology*, *21*(12), 818–832.

Madhani, H. D. (2021). Unbelievable but true: Epigenetics and chromatin in fungi. *Trends in Genetics: TIG*, *37*(1), 12–20.

McInnes, E. F., Papineni, S., Rinke, M., Schorsch, F., & Marxfeld, H. A. (2023). Agrochemicals. In *Haschek and Rousseaux's Handbook of Toxicologic Pathology, Volume 3* (pp. 727–763). Elsevier.

Mendiburu, F. (2023, October 22). *agricolae package - RDocumentation*. https://www.rdocumentation.org/packages/agricolae/versions/1.3-7

Miedaner, T., Cumagun, C. J. R., & Chakraborty, S. (2008). Population Genetics of Three Important Head Blight Pathogens *Fusarium graminearum, F. pseudograminearum* and *F. culmorum*. *Journal of Phytopathology (1986)*, *156*(3), 129–139.

*Mutect2*. (2025). GATK. https://gatk.broadinstitute.org/hc/en-us/articles/360037593851-Mutect2
O'Kane, C. J., Weild, R., & M Hyland, E. (2020). Chromatin Structure and Drug Resistance in *Candida spp*. *Journal of Fungi (Basel, Switzerland)*, *6*(3), 121.

Parker, J. E., Warrilow, A. G. S., Cools, H. J., Fraaije, B. A., Lucas, J. A., Rigdova, K., Griffiths, W. J., Kelly, D. E., & Kelly, S. L. (2013). Prothioconazole and prothioconazole-desthio activities

against *Candida albicans* sterol 14-α-demethylase. *Applied and Environmental Microbiology*, *79*(5), 1639–1645.

Parker, J. E., Warrilow, A. G. S., Cools, H. J., Martel, C. M., Nes, W. D., Fraaije, B. A., Lucas, J. A., Kelly, D. E., & Kelly, S. L. (2011). Mechanism of binding of prothioconazole to *Mycosphaerella graminicola* CYP51 differs from that of other azole antifungals. *Applied and Environmental Microbiology*, *77*(4), 1460–1465.

Powell, A. J., & Vujanovic, V. (2021). Evolution of Fusarium Head Blight Management in Wheat: Scientific Perspectives on Biological Control Agents and Crop Genotypes Protocooperation. *Applied Sciences*, *11*(19), 8960.

Price, C. L., Parker, J. E., Warrilow, A. G. S., Kelly, D. E., & Kelly, S. L. (2015). Azole fungicides - understanding resistance mechanisms in agricultural fungal pathogens. *Pest Management Science*, *71*(8), 1054–1058.

*Prosaro® PRO Fungicide*. (n.d.). Retrieved July 28, 2025, from https://www.cropscience.bayer.ca/d/fungicide-bcs-prosaro-pro-en-ca

Qian, H., Du, J., Chi, M., Sun, X., Liang, W., Huang, J., & Li, B. (2018). The Y137H mutation in the cytochrome P450 FgCYP51B protein confers reduced sensitivity to tebuconazole in *Fusarium graminearum*. *Pest Management Science*, *74*(6), 1472–1477.

Rayko, B., Ursula, H., Petr, K., Holger, B. D., & Wirsel, S. G. R. (2010). Adaptation of *Fusarium graminearum* to TebuconazoleYielded Descendants Diverging for Levels of Fitness,Fungicide Resistance, Virulence, and Mycotoxin Production. *Phytopathology*, *100*(5), 444–453.

Sandra, L. M.-R. b., Schmale III a, D., Shields c, E. J., & Bergstrom a, G. C. (2005). The relative abundance of viable spores of *Gibberella zeae* in the planetary boundary layer suggests the role of long-distance transport in regional epidemics of Fusarium head blight. *Agricultural and Forest Meteorology*, *132*(1-2), 20–27.

Schoustra, S. E., Debets, A. J. M., Slakhorst, M., & Hoekstra, R. F. (2006). Reducing the cost of resistance; experimental evolution in the filamentous fungus *Aspergillus nidulans*. *Journal of Evolutionary Biology*, *19*(4), 1115–1127.

Seong, K.-Y., Zhao, X., Xu, J.-R., Güldener, U., & Kistler, H. C. (2008). Conidial germination in the filamentous fungus *Fusarium graminearum*. *Fungal Genetics and Biology: FG & B*, *45*(4), 389–399.

Sevastos, A., Markoglou, A., Labrou, N. E., Flouri, F., & Malandrakis, A. (2016). Molecular characterization, fitness and mycotoxin production of *Fusarium graminearum* laboratory strains resistant to benzimidazoles. *Pesticide Biochemistry and Physiology*, *128*, 1–9.

Sharma, T., Sridhar, P. S., Blackman, C., Foote, S. J., Allingham, J. S., Subramaniam, R., & Loewen, M. C. (2022). *Fusarium graminearum* Ste3 G-protein coupled receptor: A mediator of hyphal chemotropism and pathogenesis. *mSphere*, *7*(6), e0045622.

Shishatskaya, E., Menzyanova, N., Zhila, N., Prudnikova, S., Volova, T., & Thomas, S. (2018). Toxic effects of the fungicide tebuconazole on the root system of *fusarium*-infected wheat plants. *Plant Physiology and Biochemistry : PPB*, *132*, 400–407.

Smith, W. G. (2022). *Diseases of field and garden crops: Chiefly such as are caused by fungi (classic reprint)*. Forgotten Books.

Syvolos, Y., Salama, O. E., & Gerstein, A. C. (2024). Constraint on boric acid resistance and tolerance evolvability in *Candida albicans*. *Canadian Journal of Microbiology*, *70*(9), 384–393.

Taxvig, C., Vinggaard, A. M., Hass, U., Axelstad, M., Metzdorff, S., & Nellemann, C. (2008). Endocrine-disrupting properties in vivo of widely used azole fungicides. *International Journal of Andrology*, *31*(2), 170–177.

Toda, M., Beer, K. D., Kuivila, K. M., Chiller, T. M., & Jackson, B. R. (2021). Trends in agricultural triazole fungicide use in the United States, 1992-2016 and possible implications for antifungal-resistant fungi in human disease. *Environmental Health Perspectives*, *129*(5), 55001.
Trail, F. (2009). For blighted waves of grain: *Fusarium graminearum* in the postgenomics era. *Plant Physiology*, *149*(1), 103–110.

*USADELLAB.org - Trimmomatic: A flexible read trimming tool for Illumina NGS data*. (n.d.). Retrieved April 27, 2025, from http://www.usadellab.org/cms/?page=trimmomatic

Vivas, R., Barbosa, A. A. T., Dolabela, S. S., & Jain, S. (2019). Multidrug-resistant bacteria and alternative methods to control them: An overview. *Microbial Drug Resistance (Larchmont, N.Y.)*, *25*(6), 890–908.

Wang, L., Wang, H., Liu, Z., Chen, Y., & Ma, Z. (2025). Priming enhances tolerance of *Fusarium graminearum* to triazole. *Pesticide Biochemistry and Physiology*, *209*(106333), 106333.
Wong, K. H., Todd, R. B., Oakley, B. R., Oakley, C. E., Hynes, M. J., & Davis, M. A. (2008). Sumoylation in *Aspergillus nidulans*: sumO inactivation, overexpression and live-cell imaging. *Fungal Genetics and Biology: FG & B*, *45*(5), 728–737.

Zhou, Y., Liao, M., Zhu, C., Hu, Y., Tong, T., Peng, X., Li, M., Feng, M., Cheng, L., Ren, B., & Zhou, X. (2018). ERG3 and ERG11 genes are critical for the pathogenesis of *Candida albicans* during the oral mucosal infection. *International Journal of Oral Science*, *10*(2). https://doi.org/10.1038/s41368-018-0013-2

Ziogas, B. N., & Malandrakis, A. A. (2015). Sterol Biosynthesis Inhibitors: C14 Demethylation (DMIs). In *Fungicide Resistance in Plant Pathogens* (pp. 199–216). Springer Japan.

# Supplementary figures and tables:

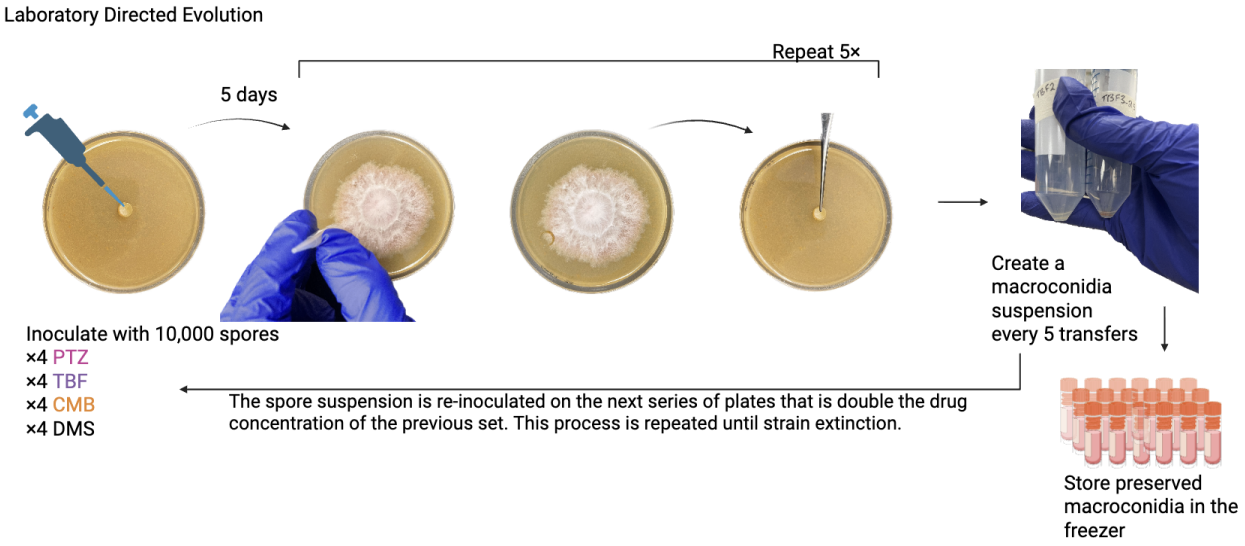


**Supporting Data Figure S1. Methodology illustration of the laboratory directed evolution workflow.**

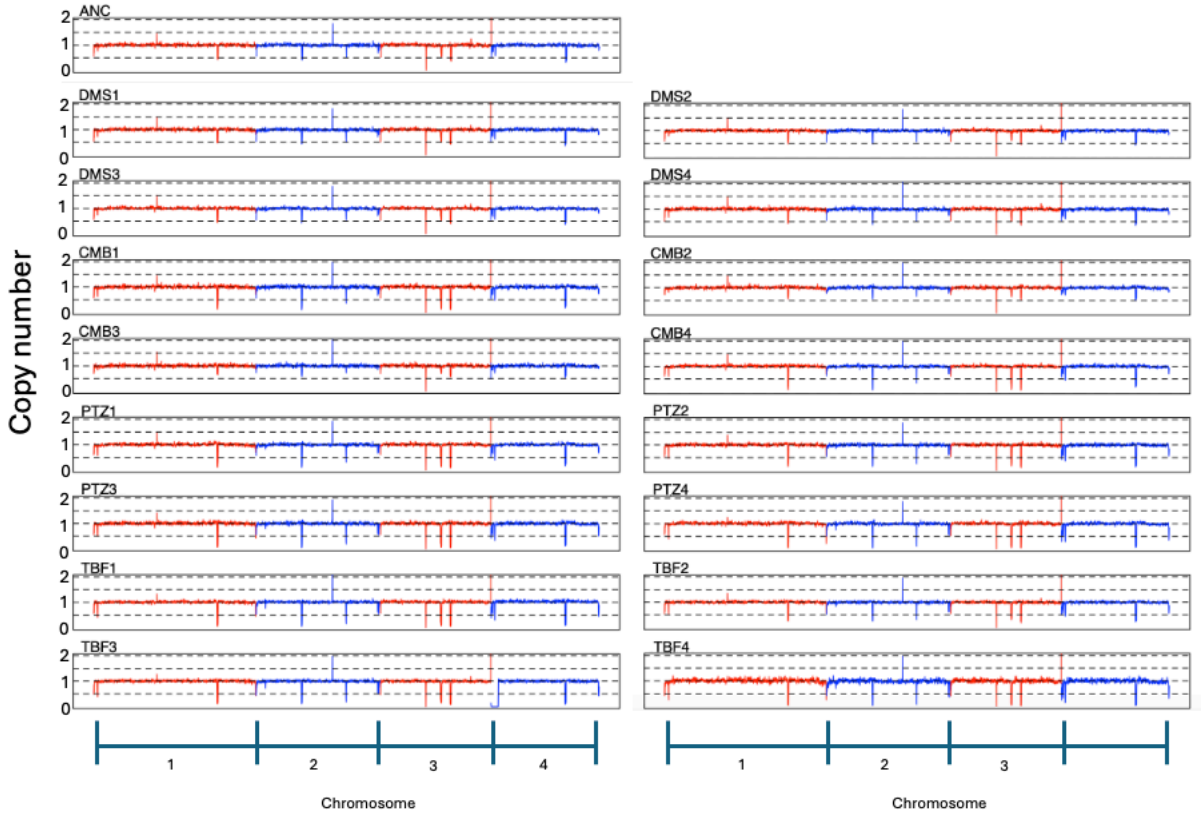


**Supporting Data Figure S2.** A visualization of the read coverage/depth throughout the genome. There was no significant variation across evolved strains compared to the ancestral strain. Chromosomes 1-4 are shown in alternating colours. Peaks correspond to repetitive regions, particularly near the telomeres.

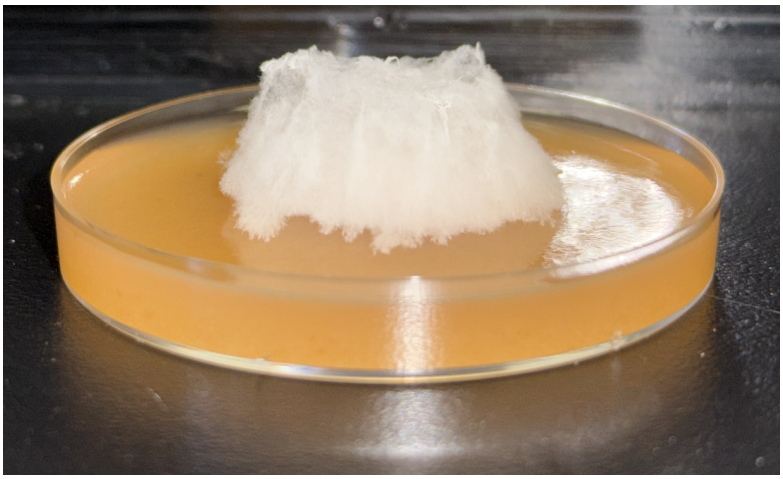

**Supporting Data Figure S3.** Upwards mycelial growth exhibited by *F. graminearum* in the presence of prothioconazole.

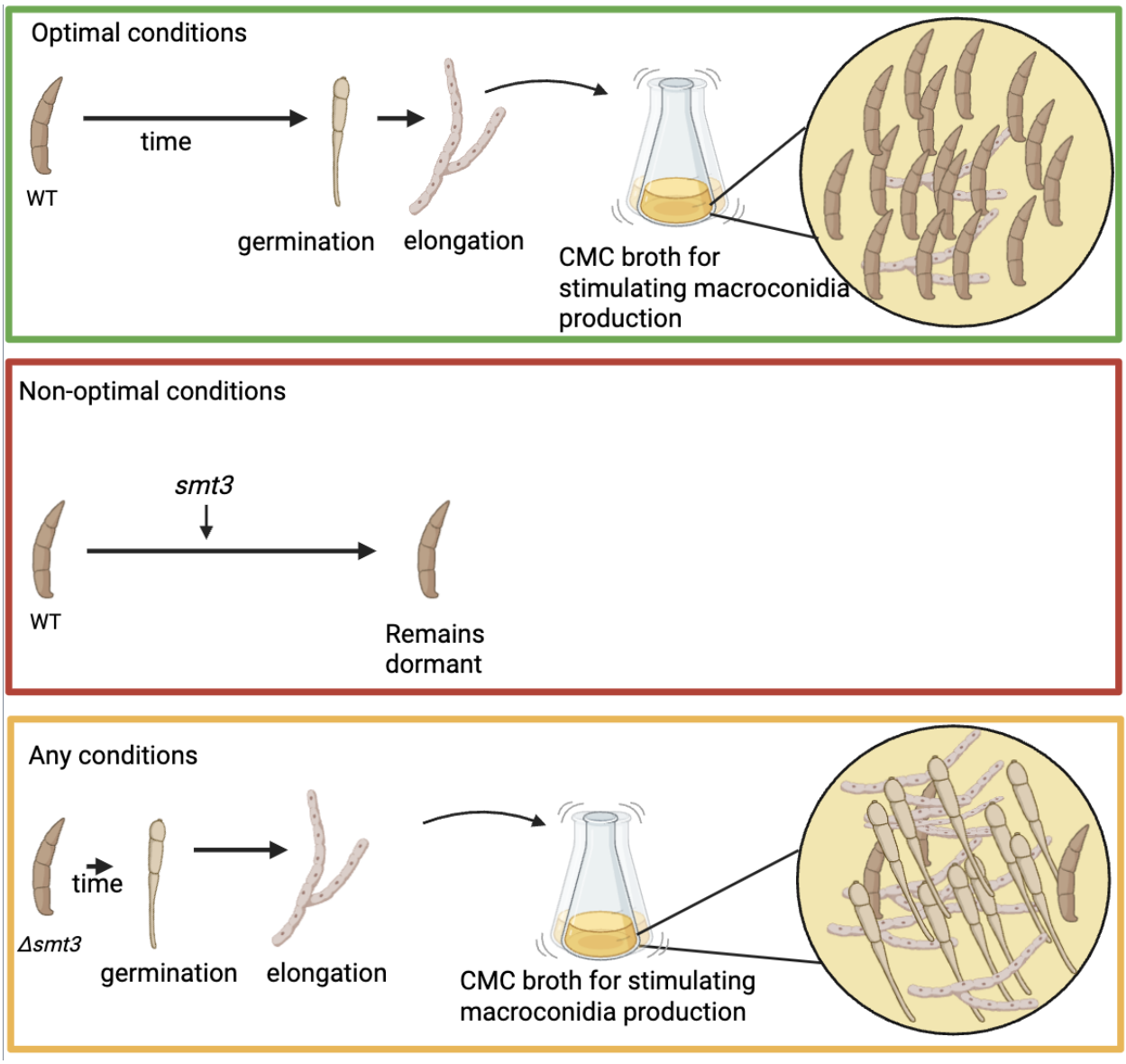


**Supporting Data Figure S4. Depiction of the characteristics of the wild type and mutant strains. Under optimal conditions, the wildtype strain will proceed from macroconidia to germination, and CMC broth will stimulate the production of macroconidia. Under non-optimal conditions, the wildtype will remain dormant until optimal conditions arise. Under any conditions, the mutant strain will initiate germination immediately, and proceed with mycelial elongation. In CMC broth, macroconidia are generated, but germinate immediately.**

# Supporting tables

**Supporting Table S2. Primers and oligos that were used in this work.**

| Name | Sequence | Use |
|---|---|---|
| 5’ HRT | TTTTGCGATTTCGATCCGCAA TCTCTCAGCCTTGCTCGACAG AAGATGATATTGAAGGAGCA CTTTTTGGGC | Amplify the hygromycin resistance gene while adding overhangs with homology to the cut site at the 5’ end of the *smt3* gene. The underlined section is homologous with the hygromycin resistance gene. |
| 3’ HRT | TCCAAAATTGTACAACGCTTT GTGAAATAGCACCGCTATTC CTTTGCCCTCGGACGAGTGCT GGGGCGTCGG | Amplify the hygromycin resistance gene while adding overhangs with homology to the cut site at the 3’ end of the *smt3* gene. The underlined section is homologous with the hygromycin resistance gene. |
| 5’ crRNA protospacer | CGCAATCTCTCAGCCTTGCA | Component of the gRNA, directing Cas9 to cut at the 5’ end of the *smt3* gene. |
| 3’ crRNA protospacer | CTTGACGACACGCATTTAGA | Component of the gRNA, directing Cas9 to cut at the 3’ end of the *smt3* gene. |
| Hygromycin_F | GGTCATTGACTGGAGCGAGG | qPCR amplification for confirming a single insertion of the hygromycin resistance gene. |

| Name | Sequence | Use |
|---|---|---|
| Hygromycin_R | ATCAGGTCGGAGACGCTGTC | qPCR amplification for confirming a single insertion of the hygromycin resistance gene. |
| FgTRI6_5 | GGCAAGACAAGGAAGGACAA | qPCR amplification of the known TRI6 gene as an acting control for gene copy number. |
| FgTRI6_3 | CGATCCCTCGTCAACACTTATG | qPCR amplification of the known TRI6 gene as an acting control for gene copy number. |
| smt3_f | CATCAAAGCCCTTGCCAAC | qPCR amplification of the smt3 gene to confirm the presence or absence of it in the knockout strains. |
| smt3_r | CTCGTGTTCACGTTCATGTTG | qPCR amplification of the smt3 gene to confirm the presence or absence of it in the knockout strains. |